Lattice Boltzmann models based on Gauss quadratures

Victor E. Ambruș

[1] Department of Physics, West University of Timișoara
Bd. Vasile Parvan 4, RO 300223 Timișoara, Romania

[2] Centre for Fundamental and Advanced Technical Research, Romanian Academy
Bd. Mihai Viteazul 24, RO 300223 Timișoara, Romania

Lattice Boltzmann 2016 workshop, University Tor Vergata, Rome
09/06/2016

Team

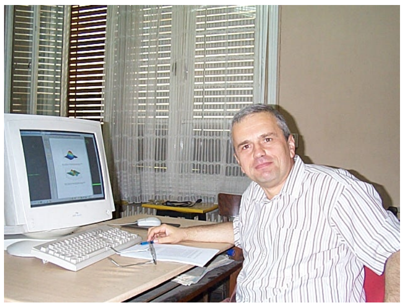
Victor Sofonea[1]


Artur Cristea[1]


Adrian Neagu[2]


Victor Ambruș[1,3]


Sergiu Busuioc[1,3]


Tonino Biciușcă[1]


Robert Blaga[3]


Adrian Horga[1]

[1]Centre for Fundamental and Advanced Technical Research, Romanian Academy
[2]Victor Babeș University of Medicine and Pharmacy Timisoara, Romania
[3]Department of Physics, West University of Timișoara, Romania

Outline

1. The Boltzmann equation
   - Moments of f
   - Chapman-Enskog expansion
2. Lattice Boltzmann models
   - Moment-matching
   - Gauss quadratures
   - Half-range quadratures
3. Conclusion

The Boltzmann distribution function

- Evolution equation of the one-particle distribution function $f \equiv f(\mathbf{x}, \mathbf{p}, t)$:

$$\partial_t f + \frac{1}{m}\mathbf{p} \cdot \nabla f + \mathbf{F} \cdot \nabla_{\mathbf{p}} f = J[f].$$

- The BGK approximation[1] is often used for the collision operator $J[f]$:

$$J_{\mathrm{BGK}}[f] = -\frac{1}{\tau}(f - f^{(\mathrm{eq})}).$$

where $\tau \sim \mathrm{Kn}/n$ is the relaxation time and $f^{(\mathrm{eq})}$ is the equilibrium distribution (D is the number of space dimensions):

$$f^{(\mathrm{eq})}(\mathbf{x}, \mathbf{p}, t) = \frac{n}{(2\pi m K_B T)^{\frac{D}{2}}} \exp\left[-\frac{(\mathbf{p} - m\mathbf{u})^2}{2mK_B T}\right].$$

[1] P. L. Bhatnagar, E. P. Gross, M. Krook, Phys. Rev. **94** (1954) 511.

Moments of f

- Macroscopic properties given as moments of order s of f:

$s=0$: number density: $$n = \int d^D p f,$$

$s=1$: velocity: $$\mathbf{u} = \frac{1}{nm} \int d^D p f \, \mathbf{p},$$

$s=2$: temperature: $$T = \frac{2}{Dn} \int d^D p f \, \frac{\boldsymbol{\xi}^2}{2m}, \qquad (\boldsymbol{\xi} = \mathbf{p} - m\mathbf{u}),$$

viscous tensor: $$\sigma_{\alpha\beta} = \int d^D p \, \frac{\xi_\alpha \xi_\beta}{m} f - nT\delta_{\alpha\beta},$$

$s=3$: heat flux: $$\mathbf{q} = \int d^D p f \, \frac{\boldsymbol{\xi}^2}{2m} \frac{\boldsymbol{\xi}}{m}.$$

Transport equations

- Multiplying the Boltzmann equation:

$$\partial_t f + \frac{1}{m}\mathbf{p}\cdot\nabla f + \mathbf{F}\cdot\nabla_{\mathbf{p}} f = J[f],$$

by the collision invariants $\psi \in \{1, \mathbf{p}, E\}$ and integrating over $\mathbf{p}$ gives:

$$\partial_t n + \partial_\alpha(\rho u_\alpha) = 0,$$

$$\partial_t(\rho u_\alpha) + \partial_\beta(\rho u_\alpha u_\beta + nT\delta_{\alpha\beta} + \sigma_{\alpha\beta}) = nF_\alpha,$$

$$(\partial_t + \partial_\alpha u_\alpha)\left(\frac{3}{2}nT + \frac{\rho\mathbf{u}^2}{2}\right) + \partial_\alpha q_\alpha + \partial_\alpha\left[u_\beta\left(nT\delta_{\alpha\beta} + \sigma_{\alpha\beta}\right)\right] = nu_\alpha F_\alpha.$$

- The evolution of the moment of order s depends on the moment of order $s+1$.

Diffuse reflection boundary conditions

- The diffuse reflection boundary conditions require:

$$f(\mathbf{x}_{\mathrm{w}}, \mathbf{p}, t) = f_{\mathrm{w}}^{(\mathrm{eq})} \equiv f^{(\mathrm{eq})}(n_{\mathrm{w}}, \mathbf{u}_{\mathrm{w}}, T_{\mathrm{w}}) \qquad (\mathbf{p} \cdot \chi < 0),$$

where χ is the outwards-directed normal to the boundary.

- Requiring zero mass-flux through the boundary:

$$\int_{\mathbf{p}\cdot\chi>0} d^3p f\,(\mathbf{p}\cdot\chi) + \int_{\mathbf{p}\cdot\chi<0} d^3p f_w^{(\mathrm{eq})}\,(\mathbf{p}\cdot\chi) = 0$$

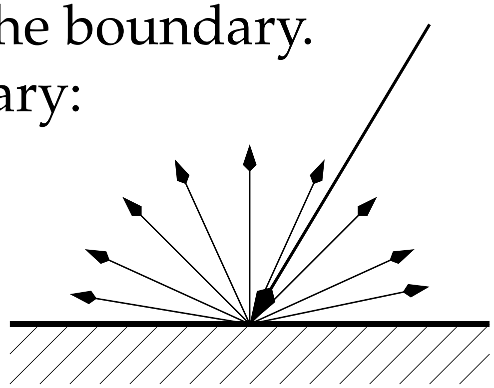

fixes the density n_{w} on the wall:

$$n_w = -\frac{\displaystyle\int_{\mathbf{p}\cdot\chi>0} d^3p f\,(\mathbf{p}\cdot\chi)}{\displaystyle\int_{\mathbf{p}\cdot\chi<0} \frac{d^Dp}{(2\pi m T_w)^{D/2}} \exp\left[-\frac{(\mathbf{p}-m\mathbf{u}_w)^2}{2mT_w}\right]}.$$

- Diffuse reflection requires the computation of integrals of f and $f^{(\mathrm{eq})}$ over half of the momentum space.

Chapman-Enskog expansion

- According to the Chapman and Enskog, f can be expanded in powers of Kn:

$$f = f^{(0)} + f^{(1)}\mathrm{Kn} + f^{(2)}\mathrm{Kn}^2 + \dots,$$

- Assuming that $\tau \sim \mathrm{Kn}$, the Boltzmann eq. can be solved iteratively:

$$f^{(0)} = f^{(\mathrm{eq})}, \qquad -\frac{\mathrm{Kn}}{\tau} f^{(1)} = \partial_{t_0} f^{(0)} + \frac{1}{m}\mathbf{p}\nabla f^{(0)} + \mathbf{F}\nabla_{\mathbf{p}} f^{(0)}, \dots$$

- $f^{(s)} = P_s(\mathbf{p}) f^{(\mathrm{eq})}$, where $P_s(\mathbf{p})$ is a polynomial of order s in $\mathbf{p}$.
- The Navier-Stokes eqs can be obtained by truncating f at $f^{(1)}$:

$$\sigma^{(1)}_{\alpha\beta} = -\frac{\tau n T}{\mathrm{Kn}}\left[\partial_\alpha u_\beta + \partial_\beta u_\alpha - \frac{2}{D}\partial_\gamma u_\gamma\right], \qquad q^{(1)}_\alpha = -\frac{1}{\mathrm{Pr}}\frac{D+2}{2m}\frac{\tau n T}{\mathrm{Kn}}\partial_\alpha T.$$

- To recover the thermal Navier-Stokes regime using BGK, the moments of $f^{(\mathrm{eq})}$ of order up to 4 are required.

Van der Waals fluids

- The Navier-Stokes equations are obtained at $O(\mathrm{Kn})$:

$$\partial_t \rho + \nabla(\rho \mathbf{u}) = 0$$
$$\rho(\partial_t \mathbf{u} + \mathbf{u}\nabla\mathbf{u}) = -\nabla p^i + \nabla(\mu(\nabla\mathbf{u} + (\nabla\mathbf{u})^T)) + \nabla(\lambda\nabla\mathbf{u}) + \rho\mathbf{F}$$

- To get the van der Waals equation of state and the surface tension, one sets

$$\mathbf{F} = \frac{1}{\rho}\nabla(p^i - p^w) + k\nabla(\Delta\rho), \qquad p^i = \rho T \qquad p^w = \frac{3\rho T}{3-\rho} - \frac{9}{8}\rho^2$$

with $\rho_c = 1$, $T_c = 1$.

Moment matching

- In lattice Boltzmann, the velocity space is replaced by a set of discrete velocities $\mathbf{p}_k$.
- The corresponding distribution function f is replaced by f_k.
- $f^{(\mathrm{eq})}$ in the collision operator is constructed such that the continuum space moments

$$\mathcal{M}^{(n)}_{\alpha_1,\alpha_2,\ldots\alpha_n} = \int d^D p\, f^{(\mathrm{eq})}\, p_{\alpha_1} p_{\alpha_2} \ldots p_{\alpha_n}$$

equal those of the discretised set $\{f_k^{(\mathrm{eq})}\}$:

$$\widetilde{\mathcal{M}}^{(n)}_{\alpha_1,\alpha_2,\ldots\alpha_n} = \sum_k f_k^{(\mathrm{eq})} p_{k,\alpha_1} p_{k,\alpha_2} \ldots p_{k,\alpha_n}$$

such that

$$\widetilde{\mathcal{M}}^{(n)}_{\alpha_1,\alpha_2,\ldots\alpha_n} = \mathcal{M}^{(n)}_{\alpha_1,\alpha_2,\ldots\alpha_n}.$$

Moments for Navier-Stokes

- The following moments of $f^{(\mathrm{eq})}$ are required to recover the Navier-Stokes equations in the isothermal limit:

$$\begin{aligned}
\sum_k f_k^{(\mathrm{eq})} &= n,\\
\sum_k f_k^{(\mathrm{eq})} p_{k,\alpha} &= \rho u_\alpha,\\
\sum_k f_k^{(\mathrm{eq})} p_{k,\alpha} p_{k,\beta} &= \rho T \delta_{\alpha\beta} + m\rho u_\alpha u_\beta,\\
\sum_k f_k^{(\mathrm{eq})} p_{k,\alpha} p_{k,\beta} p_{k,\gamma} &= m\rho T(u_\alpha \delta_{\beta\gamma} + u_\beta \delta_{\alpha\gamma} + u_\gamma \delta_{\alpha\beta}) + m^2 \rho u_\alpha u_\beta u_\gamma.
\end{aligned}$$

- Supplementary moment required for Fourier's law:

$$\sum_k f_k^{(\mathrm{eq})} p_{k,\alpha} p_{k,\beta} \mathbf{p}_k^2 = m\rho T \delta_{\alpha\beta}[(D+2)T + m\mathbf{u}^2] + m^2 \rho u_\alpha u_\beta [(D+4)T + m\mathbf{u}^2].$$

Moments of $f^{(\mathrm{eq})}$

- The moments $\mathcal{M}^{(n)}_{\alpha_1,\alpha_2,\dots\alpha_n}$ can be written as[2]:

$$\mathcal{M}^{(n)}_{\alpha_1,\alpha_2,\dots\alpha_n} = \left[\prod_{j=1}^{n}(T\partial_{u_{\alpha_j}} + mu_{\alpha_j})\right]\int d^Dp\, f^{(\mathrm{eq})}.$$
$$= \left[\prod_{j=1}^{n}(T\partial_{u_{\alpha_j}} + mu_{\alpha_j})\right] n.$$

- To correctly recover moments of $f^{(\mathrm{eq})}$ up to order N, $f_k^{(\mathrm{eq})}$ must contain at least the terms in $\mathbf{u}$ of order up to N.

[2] H. D. Chen, X. W. Shan, Physica D **237** (2008) 2003.

Polynomial form of $f^{(\mathrm{eq})}$

- $f^{(\mathrm{eq})}$ can be split as:

$$f^{(\mathrm{eq})} = nF(p)E(\mathbf{p},\mathbf{u}),$$

$$F(p) = \frac{\exp\left(-\mathbf{p}^2/2mT\right)}{(2\pi mT)^{D/2}}, \qquad E(\mathbf{p},\mathbf{u}) = \exp\left(\frac{\mathbf{p}\cdot\mathbf{u}}{T} - \frac{m\mathbf{u}^2}{2T}\right).$$

- For N'th order accuracy, E can be expanded w.r.t. $\mathbf{u}$ up to order N:

$$E^{(N)} = \sum_{j=0}^{\lfloor N/2 \rfloor} \frac{1}{j!}\left(-\frac{m\mathbf{u}^2}{2T}\right)^j \sum_{r=0}^{N-2j} \frac{1}{r!}\left(\frac{\mathbf{p}\mathbf{u}}{T}\right)^r.$$

- The momentum space can be discretised as:

$$\mathbf{p}_{ki} = p_k \mathbf{e}_{ki}, \qquad p_k = |\mathbf{p}_{ki}|, \qquad \mathbf{e}_{ki}^2 = 1.$$

- $F \to F_k$ depends only on p_k and must satisfy:

$$\sum_k F_k \sum_i p_{ki,\alpha_1} p_{ki,\alpha_2} \dots p_{ki,\alpha_s} = \begin{cases} 0 & s = 2\ell + 1, \\ (mT)^\ell \Delta_{\alpha_1 \dots \alpha_{2\ell}} & s = 2\ell. \end{cases}$$

2nd order isothermal model: D2Q9

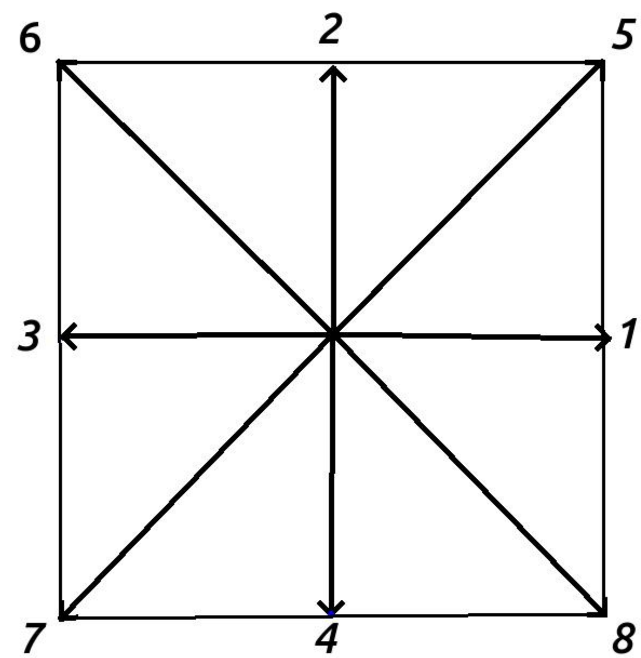

- Momentum space is discretised as:

$$p_0 = 0, \qquad p_{1,i} = (1,0)_{\rm FS}, \qquad p_{2,i} = (1,1)_{\rm FS}.$$

- $E \to E^{(2)} = 1 + \frac{\mathbf{u}\cdot\mathbf{p}}{T} + \frac{(\mathbf{u}\cdot\mathbf{p})^2}{2T^2} - \frac{m\mathbf{u}^2}{2T}.$
- F_k must satisfy the following constraints:

$$\sum_{k,i} F_k = 1 \Rightarrow F_0 + 4F_1 + 4F_2 = 1,$$

$$\sum_{k,i} F_k p_{ki,\alpha} p_{ki,\beta} = mT\delta_{\alpha\beta} \Rightarrow 2F_1 + 4F_2 = \frac{mT}{p^2},$$

$$\sum_{k,i} F_k p_{ki,\alpha} p_{ki,\beta} p_{ki,\gamma} p_{ki,\sigma} = (mT)^2 \Delta_{\alpha\beta\gamma\sigma} \Rightarrow \begin{cases} 2F_1 + 4F_2 = \frac{3(mT)^2}{p^4}, \alpha = \beta = \gamma = \sigma, \\ 4F_2 = \frac{(mT)^2}{p^4}, \alpha = \beta \neq \gamma = \sigma. \end{cases}$$

- Solution: $F_0 = \frac{4}{9}, \qquad F_1 = \frac{1}{9}, \qquad F_2 = \frac{1}{36}, \qquad T = \frac{p^2}{3m}.$

Collision-streaming: pros and cons

Pros:

- Streaming is straightforward to implement in the bulk;
- Low computational demand;
- Large time steps;

Cons:

- High order lattices are difficult to construct;
- Communication between nodes at large space separations required;
- Kinetic boundary conditions are problematic[3].

[3] J. Meng, Y. Zhang, J. Comp. Phys. **258** (2014) 601.

Finite difference LB

- Consider the equation $\partial_t q + c\partial_x q = 0$.
- The numerical solution can be written using fluxes:

$$q_i^{n+1} = q_i^n - \frac{\delta t}{\delta s}(F_{i+1/2} - F_{i-1/2}).$$

- For second order accuracy in δs, flux limiters can be used:

$$F_{i-1/2} = cq_I + \frac{1}{2}|c|\left(1 - \frac{|c|\delta t}{\delta s}\right)(f_i - f_{i-1})\psi(\theta_i),$$

$$\text{where} \qquad I = \begin{cases} i-1 & c > 0 \\ i & c < 0 \end{cases}, \qquad \theta_i = \begin{cases} \frac{f_{i-1}-f_{i-2}}{f_i - f_{i-1}} & c > 0 \\ \frac{f_{i+1}-f_i}{f_i - f_{i-1}} & c < 0 \end{cases}.$$

- ψ is the smoothness function (e.g. using MCD ≡ monitorised centred difference).
- The method works for any velocity set, provided the CFL condition is satisfied:

$$\left|\frac{c\delta t}{\delta s}\right| < 1.$$

2D Watari & Tsutahara models (N'th order accuracy)

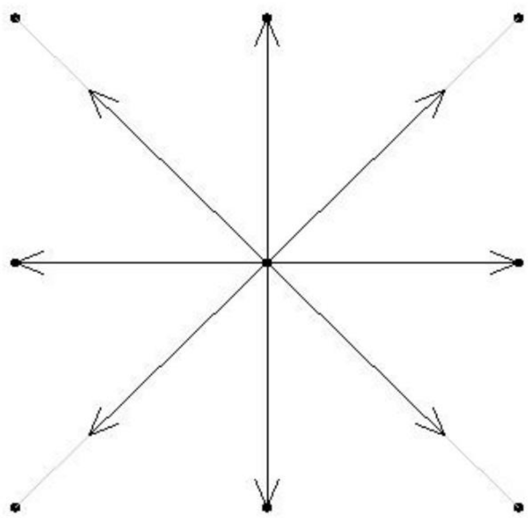

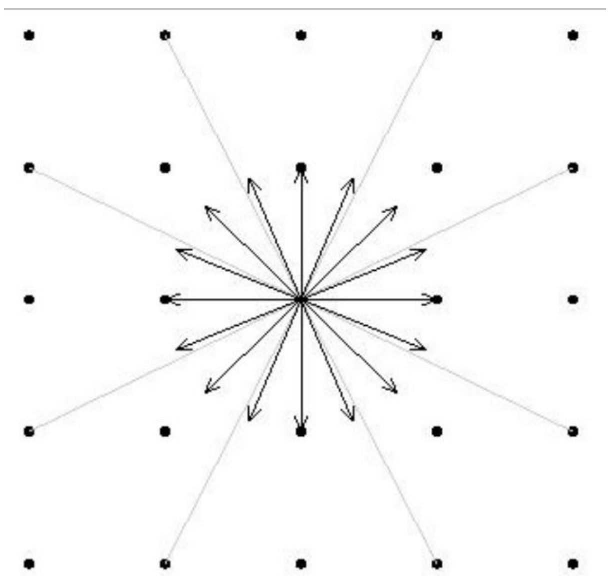

- $N + 1$ shells: $p_0 = 0, p_1, p_2, \ldots, p_N$.
- $M > 2N$ equally-spaced vectors per shell:

$$\mathbf{p}_{ki} = p_k(\cos\varphi_i, \sin\varphi_i), \qquad \varphi_i = 2\pi(i-1)/M.$$

- Extension of 5-shell model with $M = 8$.[4]

[4] M. Watari, M. Tsutahara, Phys. Rev. E **67** (2003) 036306.

Original Watari model

- For the thermal NS eqs., $N = 4$ and $M = 8$ is sufficient.
- The equations for F_k are:

$$\sum_{k,i} F_k = 1, \qquad \sum_{k,i} F_k p_k^2 = \frac{mT}{4}, \qquad \sum_{k,i} F_k p_k^4 = (mT)^2,$$
$$\sum_{k,i} F_k p_k^6 = 6(mT)^3, \qquad \sum_{k,i} F_k p_k^8 = 48(mT)^4.$$

- The solutions are:

$$F_1 = \frac{48(mT)^4 - 6(p_2^2 + p_3^2 + p_4^2)(mT)^3 + (p_2^2 p_3^2 + p_2^2 p_4^2 + p_3^2 p_4^2)(mT)^2 - \frac{p_2^2 p_3^2 p_4^2}{4}(mT)}{p_1^2 (p_1^2 - p_2^2)(p_1^2 - p_3^2)(p_1^2 - p_4^2)},$$

and similarly for F_2, F_3 and F_4, while $F_0 = 1 - 8(F_1 + F_2 + F_3 + F_4)$.

- p_k chosen such that $F_k / F_{k+1} > 1.1$ ($F_0 > 0$) for all $T_L < T < T_H$, where $T_L = 0.4$ and $T_H = 1.6$:

$$p_0 = 0, \qquad p_1 = 1.0, \qquad p_2 = 1.92, \qquad p_3 = 2.99, \qquad p_4 = 4.49.$$

Recipe for Gauss quadratures[5]

- Gauss quadratures can be used to evaluate integrals of polynomials using discrete sums:

$$\int_{\mathcal{D}} dx\, \omega(x)\, P_N(x) \simeq \sum_{k=1}^{Q} w_k P_N(x_k).$$

- The equality is exact if:
  - The order N and the number of q. points Q satisfy: $2N < Q$.
  - The q. points x_k are roots of $\phi_Q(x)$, where $\{\phi_\ell\}$ are orthogonal with respect to:

$$\int_{\mathcal{D}} dx\, \omega(x)\, \phi_\ell(x)\phi_{\ell'}(x) = \gamma_\ell \delta_{\ell\ell'}.$$

  - The quadrature weights w_k are chosen as:

$$w_k = -\frac{A_Q \gamma_Q}{A_{Q+1}\phi_{Q+1}(x_k)\phi'_Q(x_k)},$$

where A_Q is the coefficient of x^Q in $\phi_Q(x)$.

[5] F. B. Hildebrand, *Introduction to Numerical Analysis (second edition)*, Dover Publications, 1987.

Examples of Gauss quadratures[8]

- $\mathcal{D}$ and $\omega(x)$ uniquely determine the quadrature, e.g.:

	Gauss-Legendre	Gauss-Hermite	Gauss-Laguerre[6]	half-range Gauss-Hermite[7]
$\mathcal{D}$	$[-1,1]$	$(-\infty,\infty)$	$[0,\infty)$	$[0,\infty)$
$\omega(x)$	1	$e^{-x^2/2}/\sqrt{2\pi}$	$x^\alpha e^{-x}$	$e^{-x^2/2}/\sqrt{2\pi}$
ϕ_ℓ	$P_\ell(x)$	$H_\ell(x)$	$L_\ell^{(\alpha)}(x)$	$\mathfrak{h}_\ell(x)$

- Weights also determined by quadrature type:

$$w_k^P = \frac{2(1-x_k^2)}{(Q+1)^2[P_{Q+1}(x_k)]^2}, \qquad w_k^H = \frac{Q!}{[H_{Q+1}(x_k)]^2},$$

$$w_k^L = \frac{x_k\Gamma(Q+1+\alpha)}{Q!(Q+1)^2[L_{Q+1}^{(\alpha)}(x_k)]^2}, \qquad w_k^{\mathfrak{h}} = \frac{x_k a_Q^2}{\mathfrak{h}_{Q+1}^2(x_k)[x_k + \mathfrak{h}_Q^2(0)/\sqrt{2\pi}]}.$$

[6] V. E. Ambruș, V. Sofonea, Phys. Rev. E **89** (2014) 041301(R).
[7] G.P. Ghiroldi, L. Gibelli, Journal of Computational Physics **258** (2014) 568.
[8] B. Shizgal, *Spectral Methods in Chemistry and Physics: Applications to Kinetic Theory and Quantum Mechanics* (Scientific Computation), Springer, 2015.

Expansion w.r.t. orthogonal polynomials (1D)

- The construction of quadrature-based models is performed in two steps:
- 1. The discretisation of the momentum space: p_k chosen as roots of $\phi_Q(x)$ (Q is the quadrature order and $x = p, p^2, \cos\theta$, etc);
- 2. $f^{(\text{eq})}$ is truncated at order N with respect to ϕ_ℓ and $\omega(x)$:

$$f^{(\text{eq})} = \omega(x) \sum_{\ell=0}^{N} \frac{1}{\gamma_\ell} \mathcal{F}_\ell^{(\text{eq})} \phi_\ell(x), \qquad \mathcal{F}_\ell^{(\text{eq})} = \int_{\mathcal{D}} dx\, f^{(\text{eq})} \phi_\ell(x).$$

- The moments of $f^{(\text{eq})}$ can be written as:

$$\int d^3p\, f^{(\text{eq})} P_s(p) = \sum_k f_k^{(\text{eq})} P_s(p_k),$$

for all $0 \le s \le N$, where

$$f_k^{(\text{eq})} = \frac{w_k}{\omega(x)} f^{(\text{eq})}(p_k).$$

Tensor Hermite polynomials[9]

- The tensor Hermite polynomials are orthogonal on $\mathbb{R}^3_p$ w.r.t. $\omega(\mathbf{p}) = \exp(-\mathbf{p}^2/2)/(2\pi)^{D/2}$:

$$\int d^3p\, \omega(\mathbf{p}) \mathcal{H}^{(n)}_{\mathbf{i}}(\mathbf{p}) \mathcal{H}^{(m)}_{\mathbf{j}} = \delta_{mn}\delta^n_{\mathbf{ij}},$$

  where $\delta^n_{\mathbf{ij}}$ is 1 if $\mathbf{i} = (i_1, \dots i_n)$ is a permutation of $\mathbf{j}$ and 0 otherwise.
- Examples: $\mathcal{H}^{(0)} = 1, \quad \mathcal{H}^{(1)}_i = p_i, \quad \mathcal{H}^{(2)}_{ij} = p_i p_j - \delta_{ij}$, etc.
- $f^{(\mathrm{eq})}$ can be expanded as:

$$f^{(\mathrm{eq})} = \omega(\mathbf{p}) \sum_{s=0}^{N} \frac{1}{s!} \mathbf{a}^{(s)}_{\mathrm{eq}} \cdot \mathcal{H}^{(s)}(\mathbf{p}), \qquad \mathbf{a}^{(s)}_{\mathrm{eq}} = \int d^3p\, f^{(\mathrm{eq})} \mathcal{H}^{(s)}(\mathbf{p}),$$

  where $\mathbf{a}^{(0)}_{\mathrm{eq}} = n, \quad \mathbf{a}^{(1)}_{\mathrm{eq}} = \rho \mathbf{u}, \quad \mathbf{a}^{(2)}_{\mathrm{eq}} = \rho m[\mathbf{u}^2 + (T-1)\delta]$, etc.

[9] X. Shan, X.-F. Yuan, H. Chen, J. Fluid. Mech. **550** (2006) 413.

Moments and velocity set

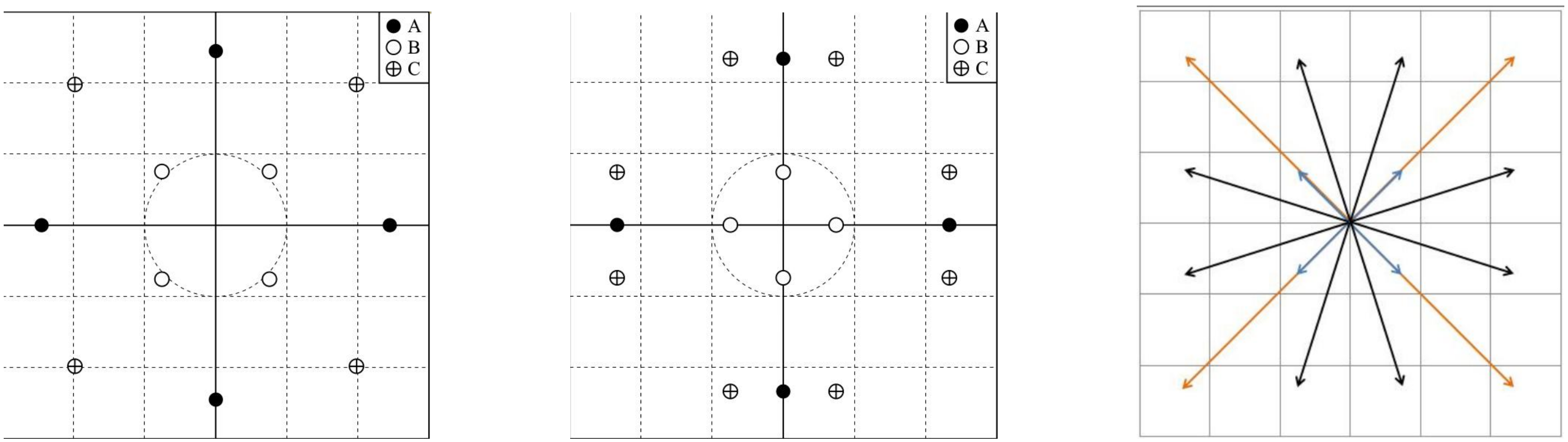

(a) (b) (c)

- The tensor Hermite approach offers access to moments

$$\mathcal{M}^{(\mathrm{eq})}_{\alpha_1,\dots\alpha_s} = \int d^3p f^{(\mathrm{eq})} p_{\alpha_1} \dots p_{\alpha_s}, \qquad (0 \le s \le N).$$

- Minimal velocity sets obtained using “moment matching”.
- (a) D2Q12 and (b) D2Q16 by A. H. Stroud (Prentice-Hall, 1971). [10]
- (c) D2Q16 as Cartesian product of 1D G-H quadratures.[11]

[10] Image from X. Shan, X.-F. Yuan, H. Chen, J. Fluid. Mech. **550** (2006) 413.

[11] Image from P. Brookes, PhD thesis, 2009.

Hermite Force term

- In the Boltzmann eq., external forces act through $\mathbf{F} \cdot \nabla_{\mathbf{p}} f$.
- In the first approximation ($f^{(\mathrm{eq})}$ force):

$$\mathbf{F} \cdot \nabla_{\mathbf{p}} f \simeq \mathbf{F} \cdot \nabla_{\mathbf{p}} f^{(\mathrm{eq})} = -\frac{1}{mT} \mathbf{F} \cdot (\mathbf{p} - m\mathbf{u}) f^{(\mathrm{eq})}. \tag{1}$$

- The *Hermite force* is constructed by taking the derivative of the expansion of f w.r.t. the Hermite polynomials:

$$f = \omega(\mathbf{p}) \sum_{n=0}^{\infty} \frac{1}{n!} \mathbf{a}^{(n)} \mathcal{H}^{(n)}(\mathbf{p}),$$

$$\nabla_{\mathbf{p}} f = -\omega(\mathbf{p}) \sum_{n=0}^{\infty} \frac{1}{n!} \mathbf{a}^{(n)} \mathcal{H}^{(n+1)}(\mathbf{p}).$$

X. Shan, X.-F. Yuan, H. Chen, J. Fluid. Mech. **550** (2006) 413.

Van der Waals phase separation[12]

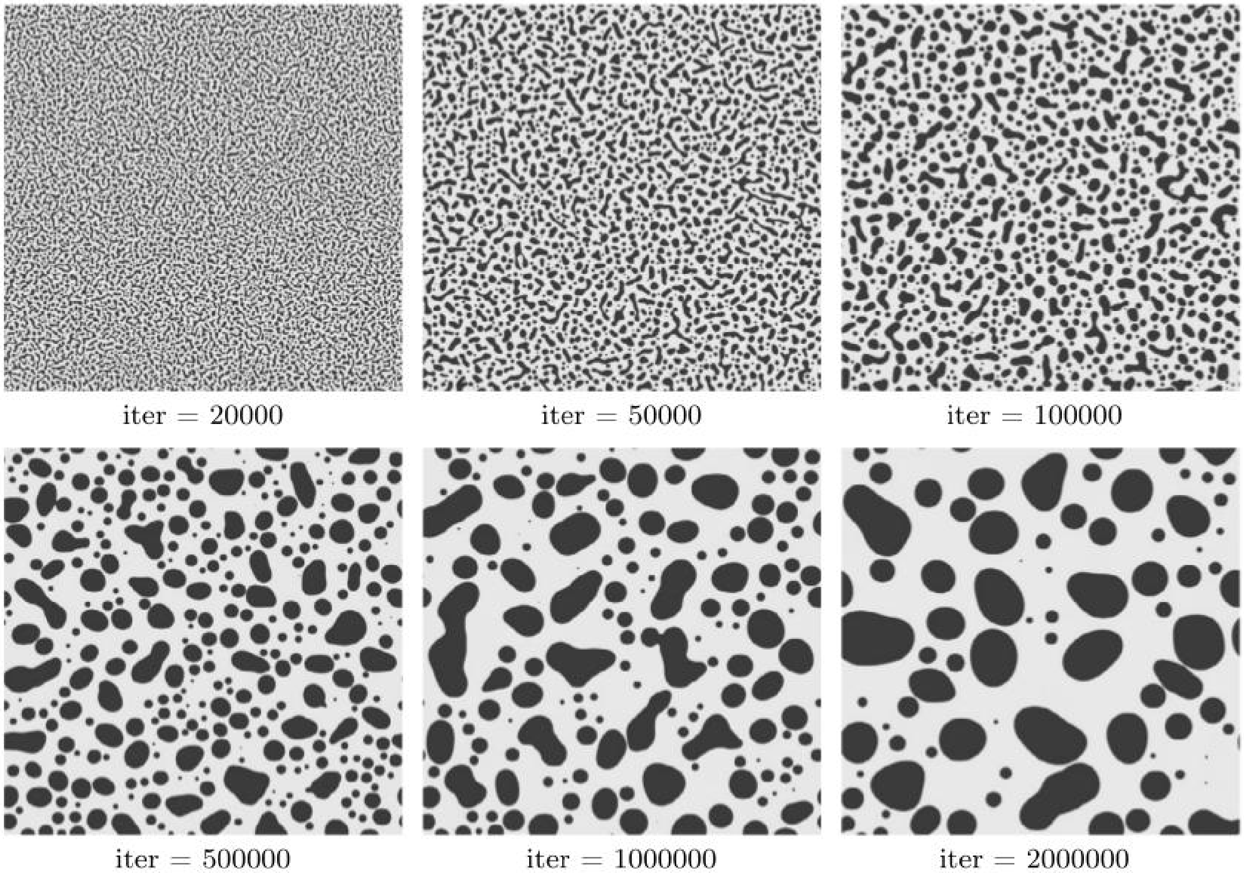

Phase separation on 4096 × 4096 nodes when $\rho_{\text{mean}} = 0.9$.

- Results obtained using $N = 3$ and the Hermite force term.
- At $t = 0$, $\rho = \rho_{\text{mean}} +$ fluctuations not exceeding 0.1%.

[12] T. Biciușcă, A. Horga, V. Sofonea, C. R. Mecanique **343** (2015) 580.

Phase diagram

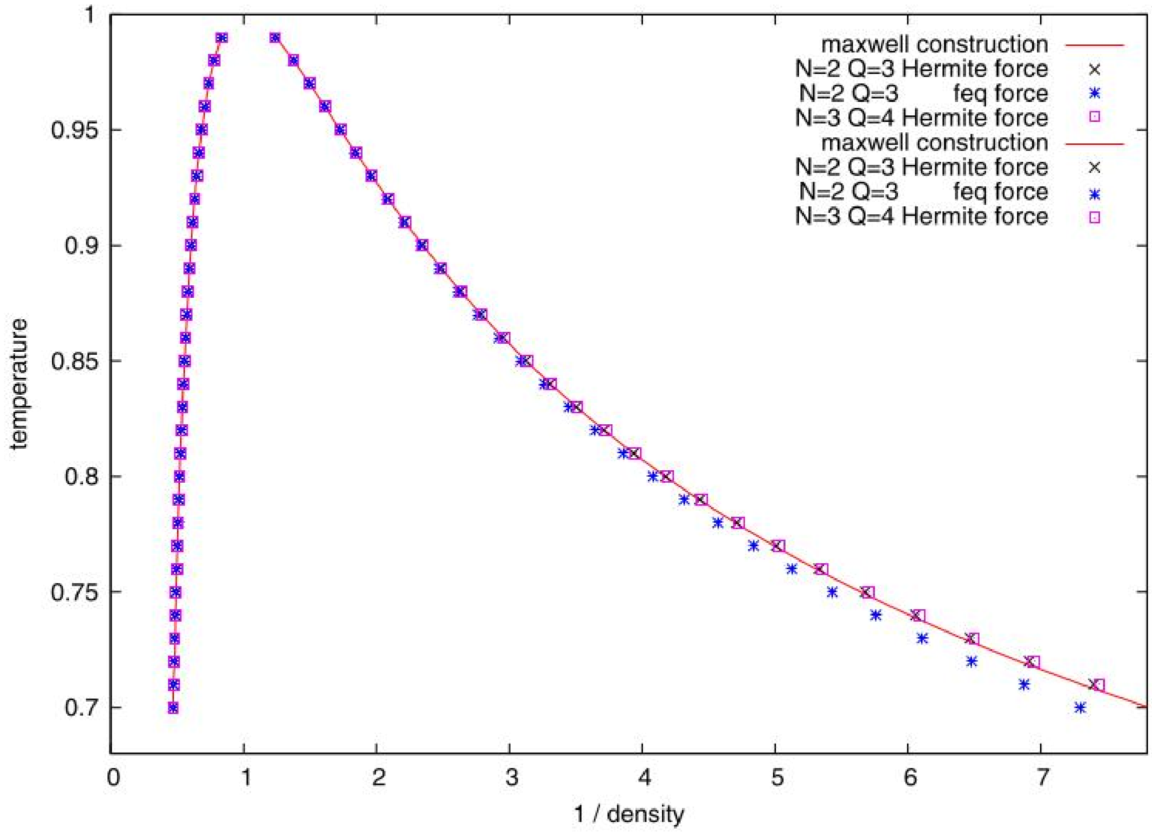

Liquid-vapour phase diagram.

- Hermite force closer to Maxwell construction than $f^{(\mathrm{eq})}$.
- $N = 2$ and $N = 3$ give similar results.

T. Biciușcă, A. Horga, V. Sofonea, C. R. Mecanique **343** (2015) 580.

Phase diagram

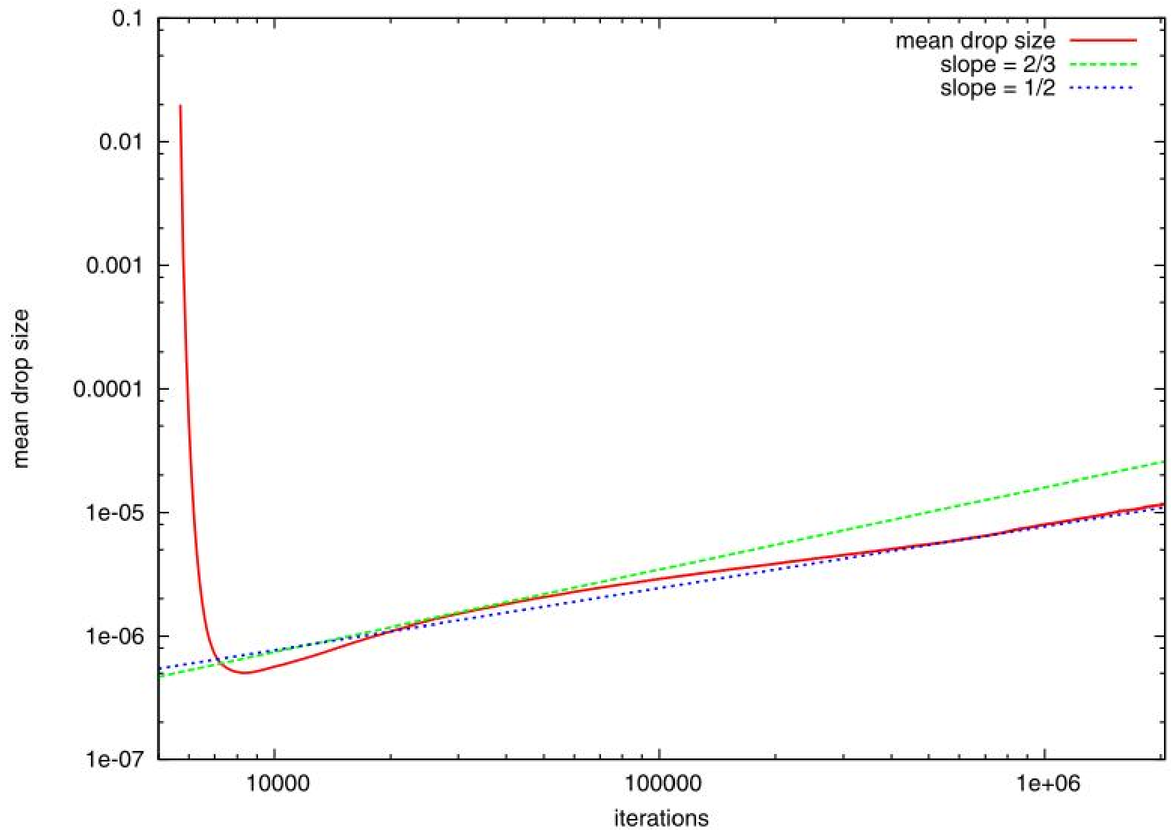

Evolution of the mean drop size $1/\mathcal{P}$ ($\mathcal{P}$ = total drop perimeter).

- Results obtained using $N = 3$ and the Hermite force term.
- Crossover between the growth exponents $2/3$ and $1/2$ confirmed.

T. Biciușcă, A. Horga, V. Sofonea, C. R. Mecanique **343** (2015) 580.

Gauss quadratures in spherical coordinates[13]

- $f^{(\mathrm{eq})} = nFE$ is expanded as:

$$E(\mathbf{p}) \rightarrow E^{(N)}(\mathbf{p}) = \sum_{j=0}^{\lfloor N/2 \rfloor} \frac{1}{j!} \left(-\frac{m\mathbf{u}^2}{2T} \right)^j \sum_{r=0}^{N-2j} \frac{1}{r!} \left(\frac{\mathbf{p}\mathbf{u}}{T} \right)^r,$$

$$F(p^2) \rightarrow F^N(p^2) = \frac{1}{\pi} e^{-p^2} \sum_{\ell=0}^{N} (1 - 2mT)^\ell L_\ell^{(1/2)}(p^2).$$

- The moments of $f^{(\mathrm{eq})}$ are obtained using spherical coordinates:

$$\int d^3p\, f^{(\mathrm{eq})} P_s(\mathbf{p}) = \sum_{k=1}^{K} \sum_{j=1}^{L} \sum_{i=1}^{M} f^{(\mathrm{eq})}_{kji} P_s(p_k, \theta_j, \varphi_i),$$

where $f^{(\mathrm{eq})} = nF_k E_{kji}$, with:

$$F_k = \frac{w_k^{(L)}}{M\sqrt{\pi}} \sum_{\ell=0}^{N} (1 - 2mT)^\ell L_\ell^{(1/2)}(p_k^2), \qquad E_{kji} = w_j^{(P)} E^{(N)}(\mathbf{p}_{kji}).$$

[13] V. E. Ambruș, V. Sofonea, Phys. Rev. E **86** (2012) 016708.

Gauss quadratures in spherical coordinates: Momentum set

- Discrete momenta $\mathbf{p}_{kji}$ have components:

$$\mathbf{p}_{kji,x} = p_k \sin\theta_j \cos\varphi_i, \qquad \mathbf{p}_{kji,y} = p_k \sin\theta_j \sin\varphi_i, \qquad \mathbf{p}_{kji,z} = p_k \cos\theta_j.$$

- The Mysovskih quadrature[14] requires that $\varphi_i = \phi + 2\pi(i-1)/M$ (ϕ is an arbitrary phase).
- According to the Gauss-Legendre requires, $z_j = \cos\theta_j$ are the L roots of $P_L(z)$
- The Gauss-Laguerre quadrature implies that $x_k = p_k^2$ are the roots of $L_K^{(1/2)}(x)$.
- For N'th order accuracy, $L > N$, $K > N$ and $M > 2N \Rightarrow$ at least $2(N+1)^3$ velocities.
- Also available for relativistic flows[15].

[14] I.P.Mysovskikh, Soviet Math. Dokl. 36, 229 (1988).

[15] P. Romatschke, M. Mendoza, S. Succi, Phys. Rev. C **84** (2011) 034903.

Example of resulting models[16]

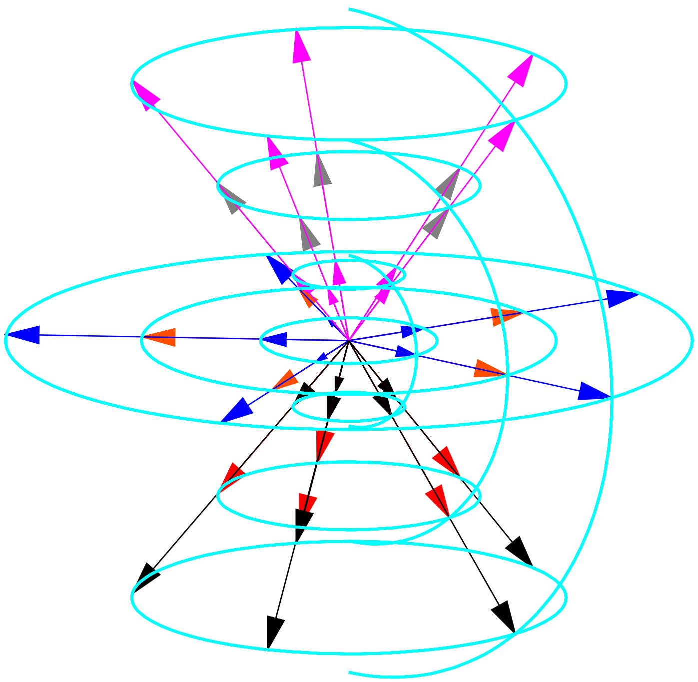

SLB(2; 3, 3, 5)

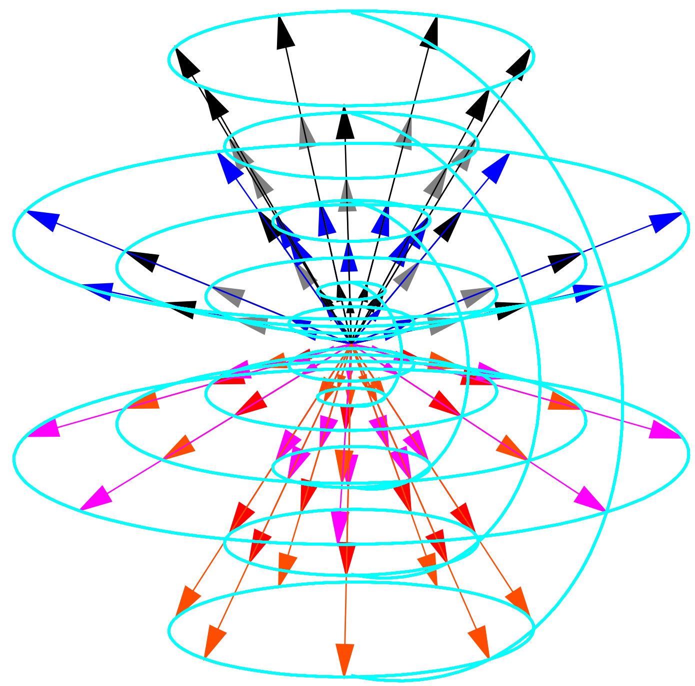

SLB(3; 4, 4, 7)

- Resulting models are labelled SLB($N; K, L, M$).

[16] V. E. Ambruș, V. Sofonea, J. Phys.: Conf. Ser. **362** (2012) 012043.

Application to Couette flow

- $3D$ flow between parallel plates ($z_+ = -z_- = -0.5$) moving along the y axis.
- Diffuse reflection on the z axis.
- $u_w \in \{0.42, 0.63\}$, $T_w = 1.0$.
- The Shakhov model was used to obtain Pr $= 2/3$.

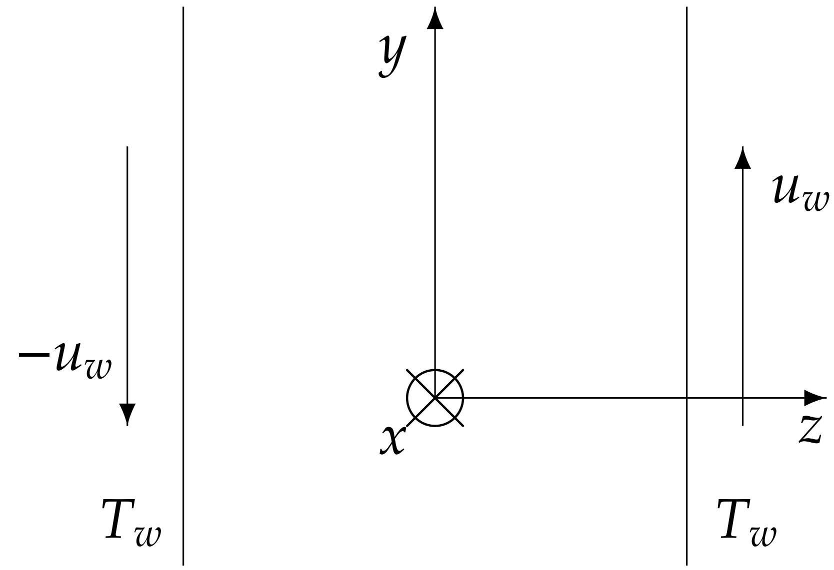

V. E. Ambruș, V. Sofonea, Phys. Rev. E **86** (2012) 016708.

Comparison to DSMC

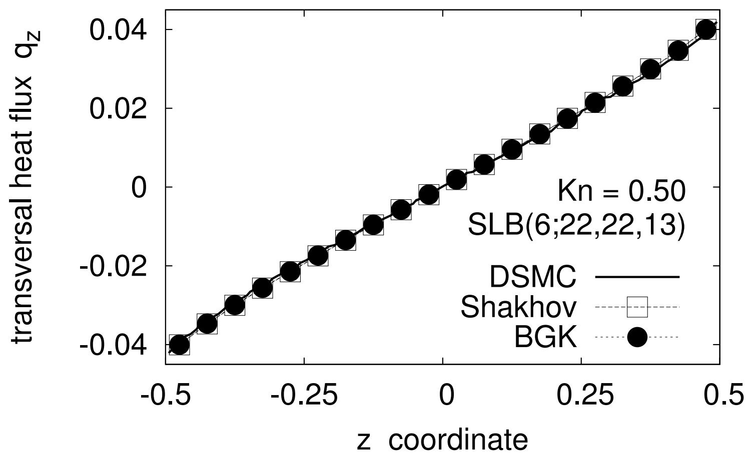

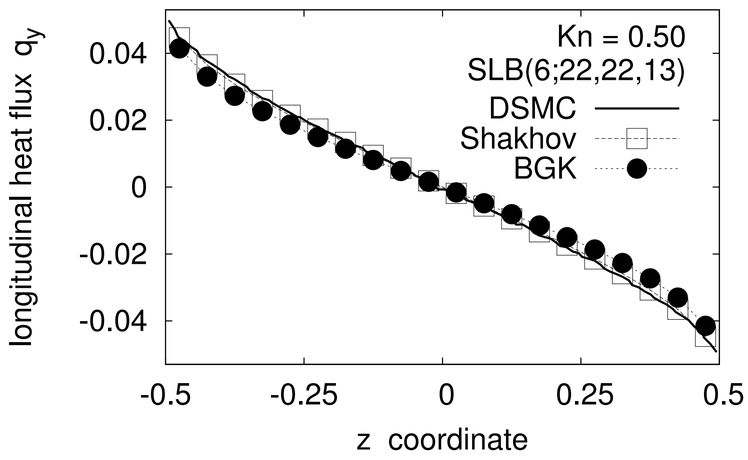

- DSMC results taken from[17].
- Good agreement observed for Shakhov up to Kn = 0.5.
- The BGK results showed a deviation in q_y at all Kn $\leq$ 0.5.

[17] M. Torrilhon, H. Struchtrup, J. Comput. Phys. **227** (2008) 1982.
V. E. Ambruș, V. Sofonea, Phys. Rev. E **86** (2012) 016708.

Comparison to DSMC[19]

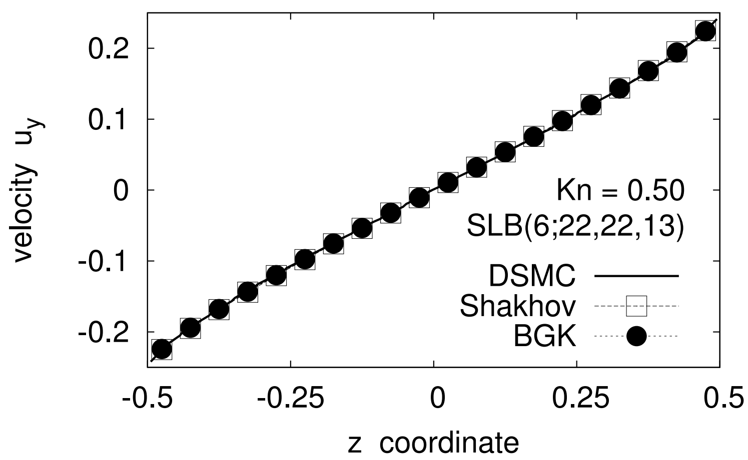

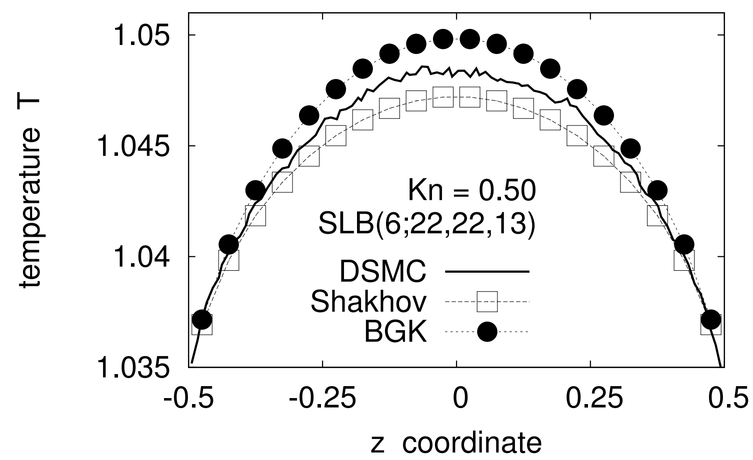

- DSMC results taken from[18].
- Slow convergence exhibited by T w.r.t. the increase of K, L and M at Kn = 0.5.
- The DSMC temperature profile is between the BGK and Shakhov results.

[18] M. Torrilhon, H. Struchtrup, J. Comput. Phys. **227** (2008) 1982.
[19] V. E. Ambruș, V. Sofonea, Phys. Rev. E **86** (2012) 016708.

Gauss-Hermite quadratures in Cartesian coordiantes

- $f^{(\mathrm{eq})} = n g_x g_y g_z$ can be factorised with respect to Cartesian coordinates:

$$g_\alpha = \frac{\exp\left[-(p_\alpha - m u_\alpha)^2/2mT\right]}{\sqrt{2\pi m T}} = \frac{e^{-\overline{p}^2/2}}{\sqrt{2\pi}} \sum_{\ell=0}^{N} \mathcal{G}_{\alpha,\ell} H_\ell(\overline{p}_\alpha),$$

where $\overline{p}_\alpha = p_\alpha / p_{0,\alpha}$ and $p_{0,\alpha}$ is the α component of some reference momentum $\mathbf{p}_0$.

- The moments of $f^{(\mathrm{eq})}$ are obtained using Cartesian coordinates, on each axis independently:

$$\int d^3p\, f^{(\mathrm{eq})} p_x^{s_x} p_y^{s_y} p_z^{s_z} \rightarrow \int_{-\infty}^{\infty} dp_\alpha g_\alpha p_\alpha^s = \sum_{k=1}^{Q_\alpha} g_{\alpha,k} p_{\alpha,k}^s,$$

where[20]

$$g_{\alpha,k} = w_{\alpha,k} \sum_{\ell=0}^{N_\alpha} H_\ell(\overline{p}_{\alpha,k}) \sum_{s=0}^{\lfloor \ell/2 \rfloor} \frac{1}{2^s s! (\ell - 2s)!} \left(\frac{mT}{p_{0,\alpha}^2} - 1\right)^s \left(\frac{m u_\alpha}{p_{0,\alpha}}\right)^{\ell - 2s}.$$

[20] V. E. Ambruș, V. Sofonea, J. Comp. Phys. **316** (2016) 1.

Gauss-Hermite quadratures: Momentum set

- The direct-product Gauss-Hermite quadrature offers access to moments:

$$\mathcal{M}^{(\mathrm{eq})}_{s_x,s_y,s_z} = \int d^3p\, f^{(\mathrm{eq})} p_x^{s_x} p_y^{s_y} p_z^{s_z},$$

  where $0 \le s_x, s_y, s_z \le N$.
- The momentum set $\mathbf{p}_{ijk} = (p_{i,x}, p_{j,y}, p_{k,z})$ is obtained as a direct product between 1D G-H quadrature points.
- For N'th order accuracy, $Q_\alpha > N \Rightarrow$ at least $(N+1)^3$ velocities.

T-junction device[21]

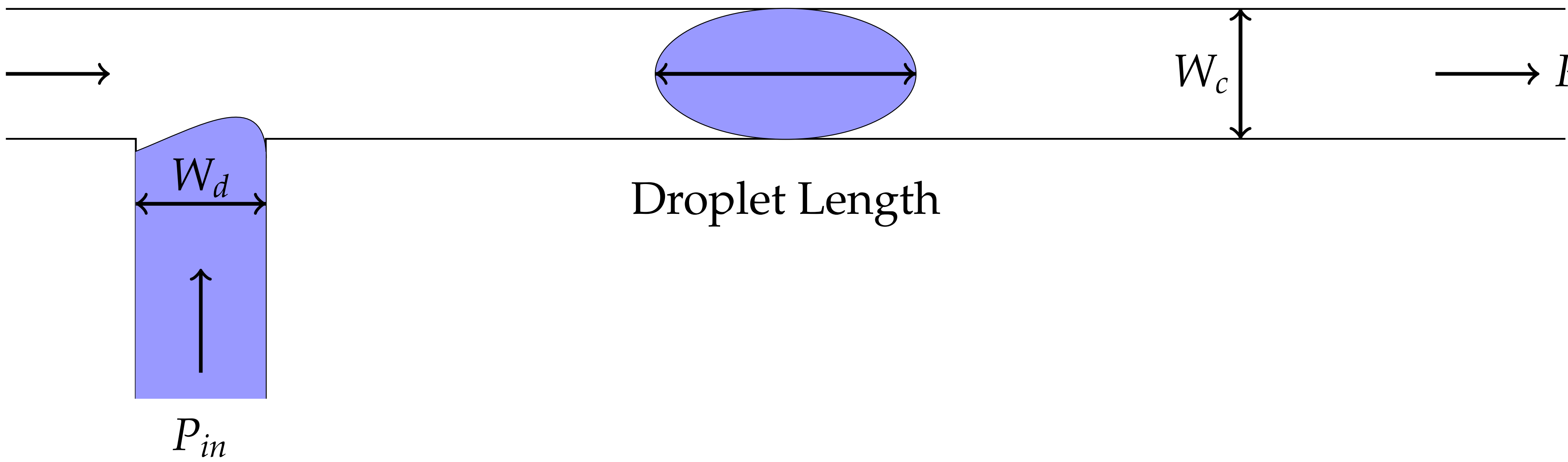

- Two inlets(liquid and vapour) and one outlet flow.
- $Z = \frac{W_c}{W_d}$ is used to characterise the geometry.
- $\Delta P = P_{in} - P_{out}$

[21] S. Busuioc,V. E. Ambruș, V. Sofonea, Presentation at TIM-2016 conference (May, 2016), Timișoara, Romania.

T-junction droplet formation regimes

Isothermal flows at $T = 0.8$ with hydrophobic surfaces.

Squeezing regime

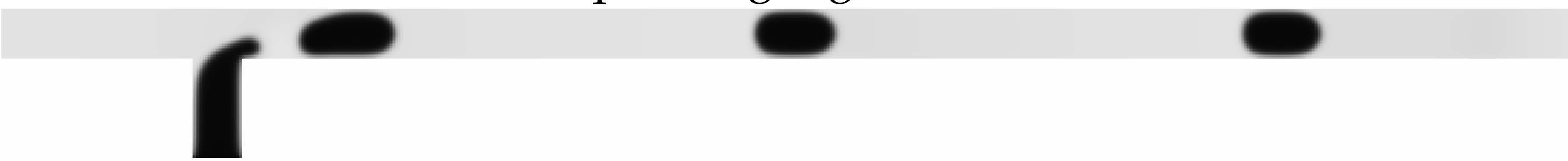

Dripping regime

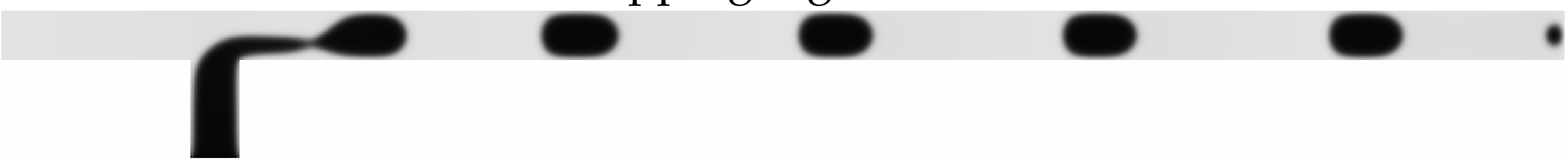

Jetting regime

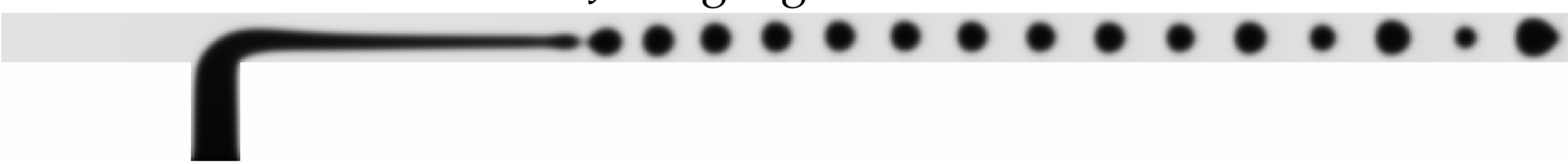

S. Busuioc, V. E. Ambruș, V. Sofonea, Presentation at TIM-2016 conference (May, 2016), Timișoara, Romania.

Droplet length as function of driving force (acceleration)

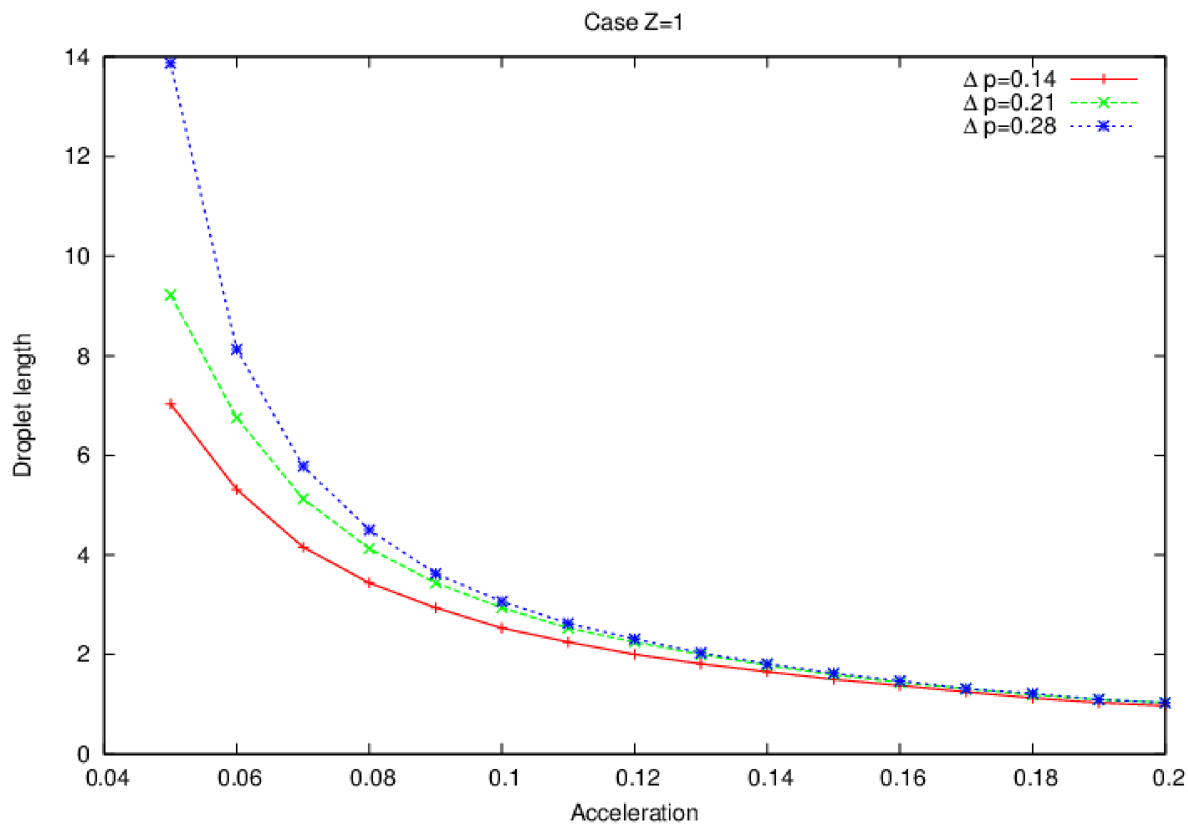

- The droplet size decreases with a_y and increases with Δp.
- For large a_y, the droplet length is less sensitive to changes in Δp.

S. Busuioc, V. E. Ambruș, V. Sofonea, Presentation at TIM-2016 conference (May, 2016), Timișoara, Romania.

Couette flow[22]

- $2D$ flow between parallel plates ($x_+ = -x_- = -0.5$) moving along the y axis.
- Diffuse reflection on the x axis.
- $u_w \in \{0.1, 0.63, 1.0\}$, $T_w = 1.0$.
- The BGK model was used.

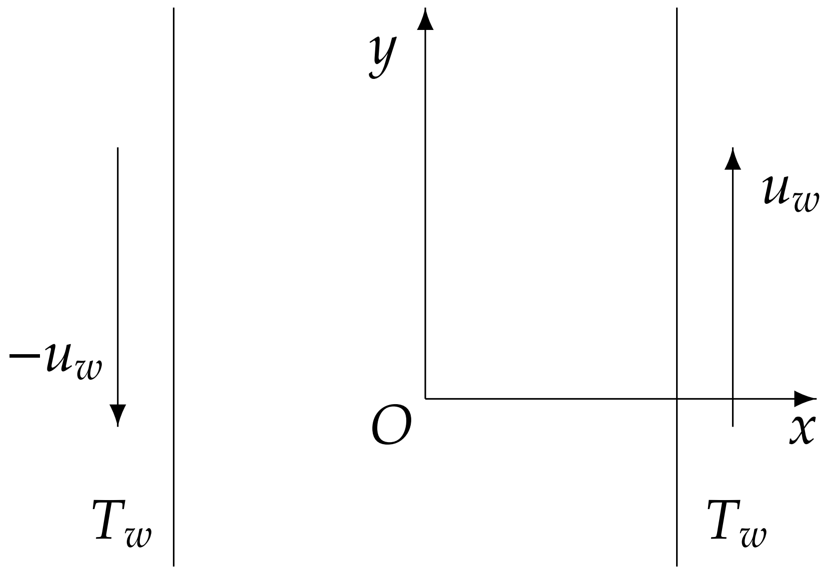

[22] V. E. Ambruș, V. Sofonea, J. Comp. Phys. **316** (2016) 1.

Convergence test

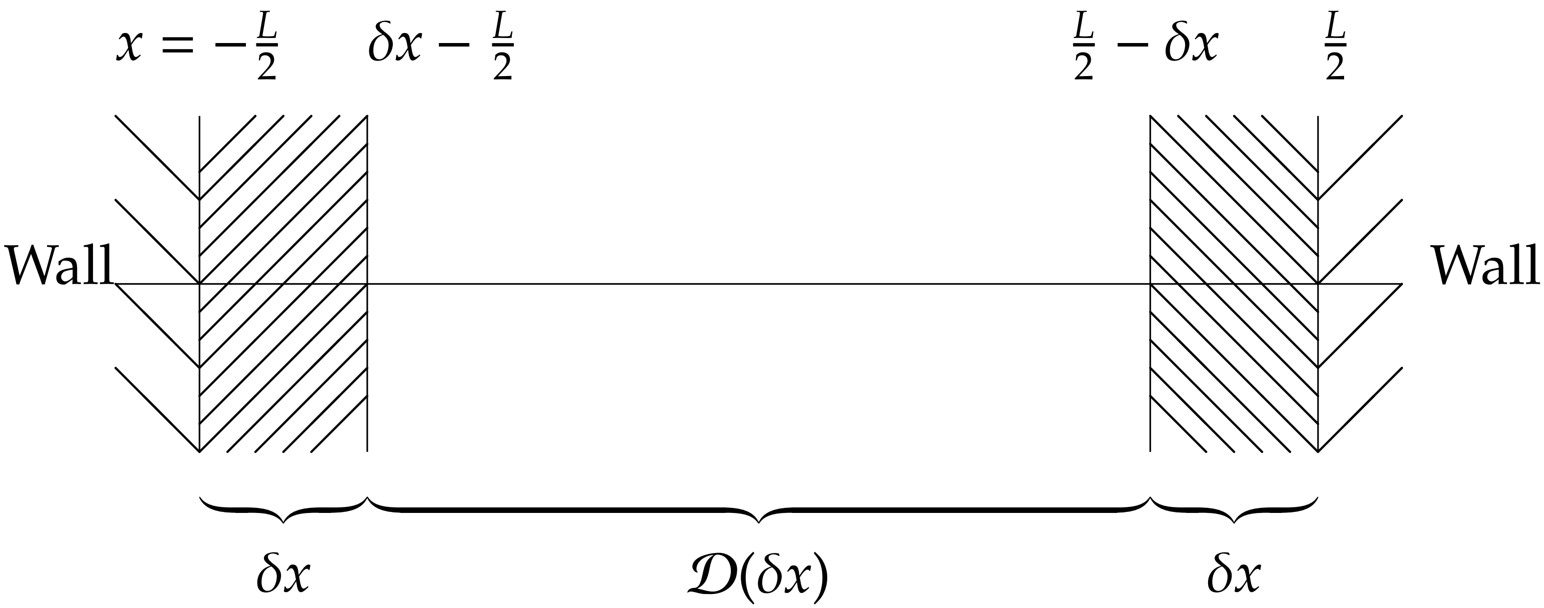

- Purpose: test the dependence of the simulation results on Q_x.

V. E. Ambruș, V. Sofonea, J. Comp. Phys. **316** (2016) 1.

Convergence test

- The following error is calculated for each profile $M \in \{n, u_y, T, q_x, q_y\}$:

$$\varepsilon_M(\delta x) = \frac{\max_{x \in \mathcal{D}(\delta x)} [M(x) - M_{\rm ref}(x)]}{\Delta M_{\rm ref}(\delta x)},$$

where $M_{\rm ref}(x)$ represents the reference profile and

$$\Delta M_{\rm ref}(\delta x) = \max\{\max_{x \in \mathcal{D}(\delta x)}[M_{\rm ref}(x)] - \min_{x \in \mathcal{D}(\delta x)}[M_{\rm ref}(x)], 0.1\}$$

- The restriction that $\Delta M_{\rm ref} \ge 0.1$ is imposed to limit the effects of numerical fluctuations for quasi-constant profiles.
- Convergence is achieved in the domain $\mathcal{D}(\delta x)$ when

$$\varepsilon(\delta x) \equiv \max_M[\varepsilon_M(\delta x)] \le 0.01.$$

V. E. Ambruș, V. Sofonea, J. Comp. Phys. **316** (2016) 1.

Convergence of HLB

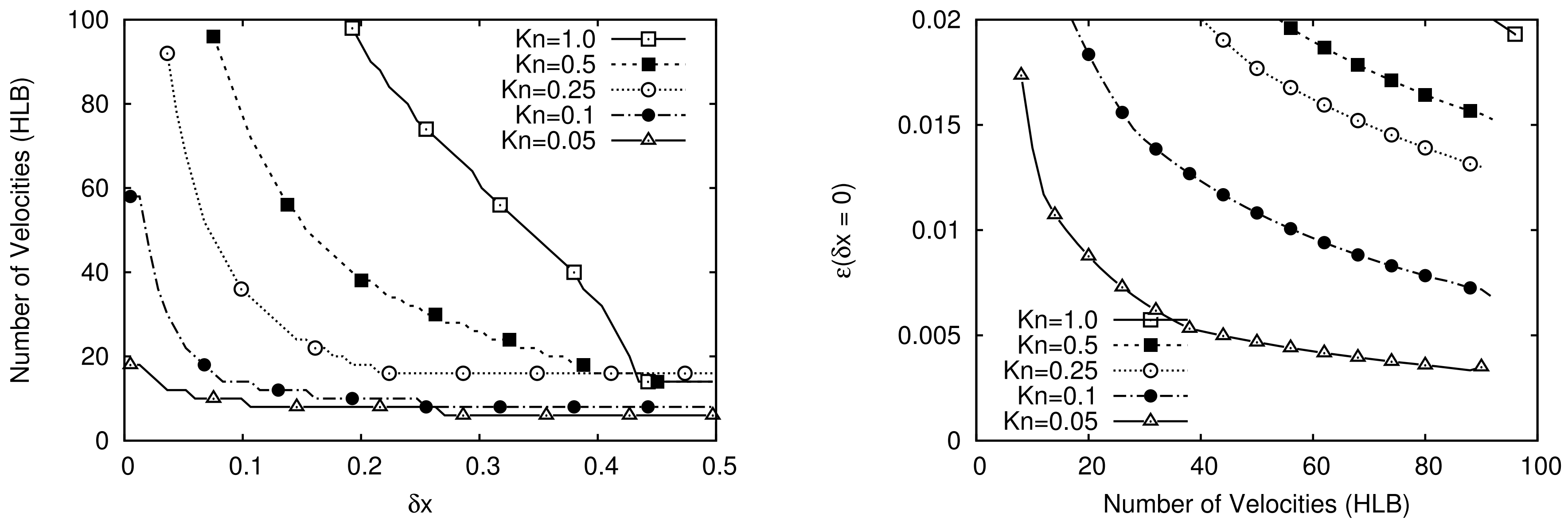

- $2D$ Couette-BGK, $u_w = 0.63$.
- Slow convergence w.r.t. the quadrature order at all non-negligible Kn.
- 1% test not satisfied for all $Q < 100$ when $\text{Kn} \gtrsim 0.25$.

V. E. Ambruș, V. Sofonea, J. Comp. Phys. **316** (2016) 1.

Formulation of the half-space problem

- Rewrite integrals over the whole momentum space in terms of half-range integrals ($\mathcal{D} = [0, \infty)$):

$$\int_{-\infty}^{\infty} dp\, g_\alpha(p_\alpha) P_n(p_\alpha) = \int_0^\infty dp_\alpha [g_\alpha(p_\alpha) P_n(p_\alpha) + f^{(\text{eq})}(-p_\alpha) P_n(-p_\alpha)],$$

- The half-range integrals can be recovered using half-range quadratures:

$$\int_0^\infty dx\, \omega(x) P_s(x) = \sum_{k=1}^{Q} w_k P_s(x_k),$$

where the quadrature is exact for $Q > 2s$.
- The q. points x_k are the Q roots of $\phi_Q(x)$.
- The polynomials $\phi_\ell(x)$ are orthogonal w.r.t. $\omega(x)$ on $\mathcal{D} = [0, \infty)$.
- The q. weights w_k can be calculated using:

$$w_k = -\frac{A_Q \gamma_Q}{A_{Q+1} \phi_{Q+1}(x_k) \phi'_Q(x_k)}.$$

Expansion of $f^{(\mathrm{eq})}$ w.r.t. half-range polys

- g_α can be expanded w.r.t. Laguerre $[\phi_\ell(x) = L_\ell(x)]$[23] or half-range Hermite $[\phi_\ell(x) = \mathfrak{h}_\ell(x)]$[24] polynomials:

$$g_{\alpha,k} = \frac{w_{\alpha,k}}{2} \sum_{s=0}^{N_\alpha} \left(\frac{mT}{2p_{0,\alpha}^2} \right)^{s/2} \Phi_s^{N_\alpha}(|\overline{p}_{\alpha,k}|) \left[(1 + \operatorname{erf} \zeta_\alpha) P_s^+(\zeta_\alpha) + \frac{2e^{-\zeta_\alpha^2}}{\sqrt{\pi}} P_s^*(\zeta_\alpha) \right],$$

where $\zeta_\alpha = \sigma_\alpha u_\alpha \sqrt{m/2T}$ and

$$\Phi_s^{N_\alpha}(|\overline{p}_{\alpha,k}|) = \sum_{\ell=s}^{N_\alpha} \frac{1}{\gamma_\ell} \phi_{\ell,s}\, \phi_\ell(|\overline{p}_{\alpha,k}|).$$

The polynomials P_s^+ and P_s^* are defined as:

$$P_s^*(\zeta_\alpha) = \sum_{j=0}^{s-1} \binom{s}{j} P_j^+(\zeta_\alpha) P_{s-j-1}^-(\zeta_\alpha), \qquad P_s^\pm(\zeta_\alpha) = e^{\mp\zeta_\alpha^2} \frac{d^s}{d\zeta_\alpha^s} e^{\pm\zeta_\alpha^2}.$$

[23] V. E. Ambruș, V. Sofonea, Phys. Rev. E **89** (2014) 041301(R)
[24] V. E. Ambruș, V. Sofonea, J. Comp. Phys. **316** (2016) 1.

Mixed LB models[25]

- Half-range quadratures are useful on directions perpendicular to walls.
- On directions having periodic boundary conditions, the full-space Hermite quadrature requires twice as less quadrature points for the same accuracy.
- Models for $2D$ flow with walls perpendicular to the x axis and periodic b.c.s along the y axis:

$$\text{HHLB}(Q_x) \times \text{HLB}(Q_y), \qquad \text{HLB}(Q_x) \times \text{HLB}(Q_y),$$

i.e. only the full-space Hermite quadrature is considered on the axis parallel to the walls.

[25] V. E. Ambruș, V. Sofonea, J. Comp. Phys. **316** (2016) 1.

Couette flow - revisited

- $2D$ flow between parallel plates ($x_+ = -x_- = -0.5$) moving along the y axis.
- Diffuse reflection on the x axis.
- $u_w \in \{0.1, 0.63, 1.0\}$, $T_w = 1.0$.
- The reference profiles were obtained using the HHLB(21) $\times$ HLB(4) model.[26]
- Good results obtained in $3D$ with the Shakhov model using the LLB models.[27]

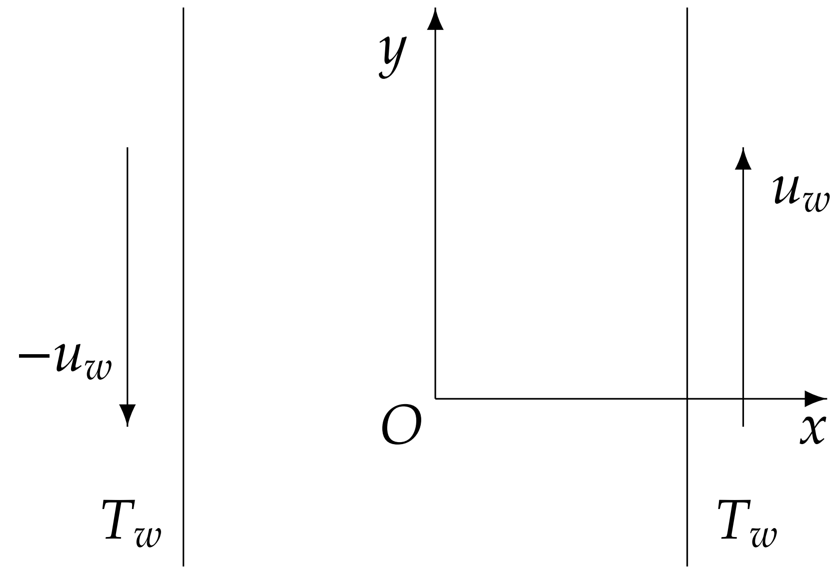

[26] V. E. Ambruș, V. Sofonea, J. Comp. Phys. **316** (2016) 1 [2D, BGK].
[27] V. E. Ambruș, V. Sofonea, Phys. Rev. E **89** (2014) 041301(R) [3D, Shakhov].

Validation

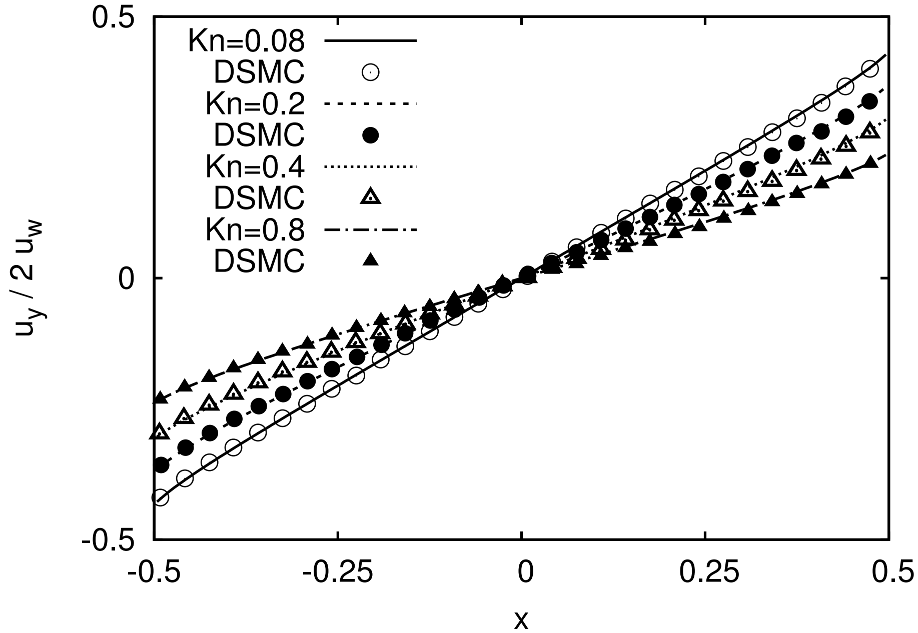

(a)

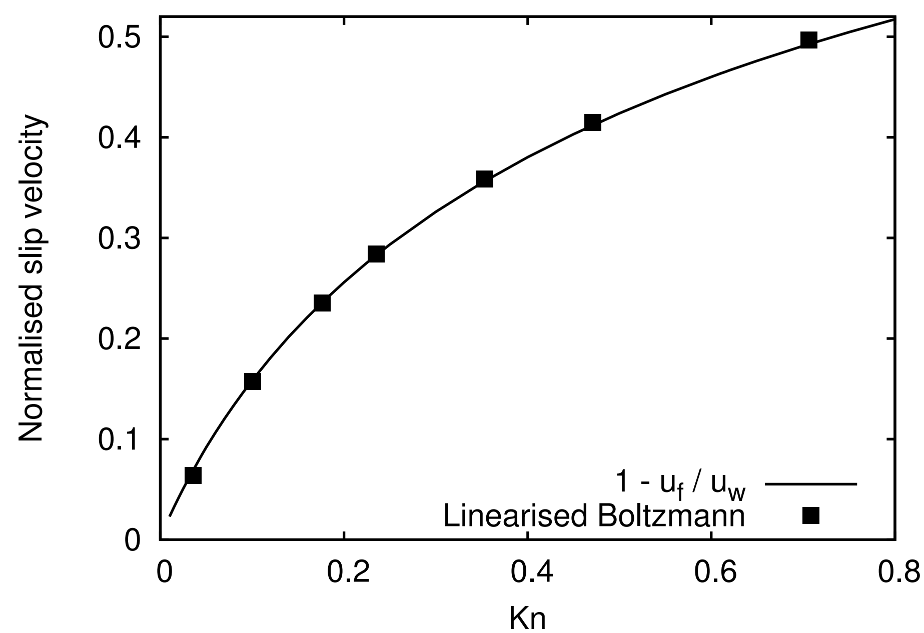

(b)

- DSMC results in (a) and linearised Boltzmann results in (b) obtained from[28].
- LB results obtained using HHLB(21) × HLB(4) are in excellent agreement with the DSMC and linearised Boltzmann results.

[28] S. H. Kim, H. Pitsch, I. D. Boyd, J. Comput. Phys. **227** (2008) 8655.

Reference profiles: T

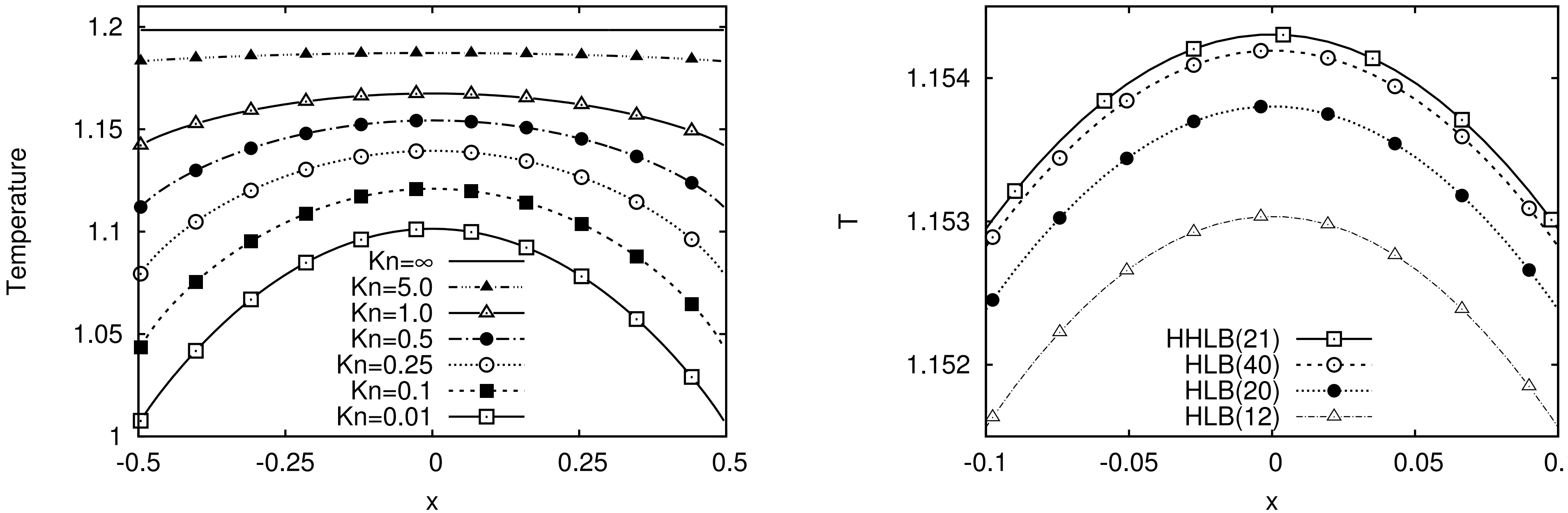

- T increases monotonically with Kn everywhere across the channel.
- $T^{\text{ballistic}} = T_w + m u_w^2 / D$.
- Reference profiles obtained using HHLB(21) × HLB(4).

V. E. Ambruș, V. Sofonea, J. Comp. Phys. **316** (2016) 1.

Reference profiles: q_x and q_y

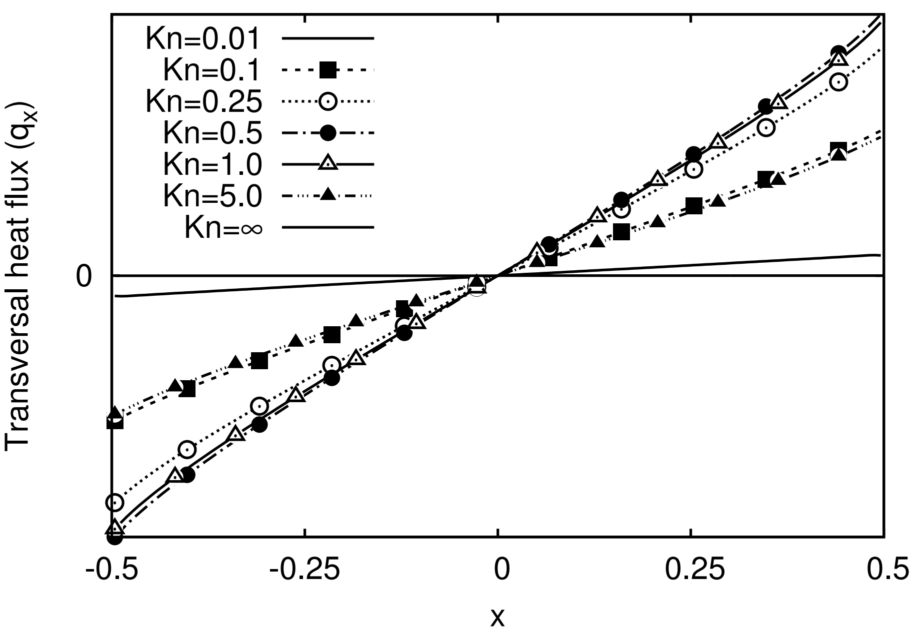

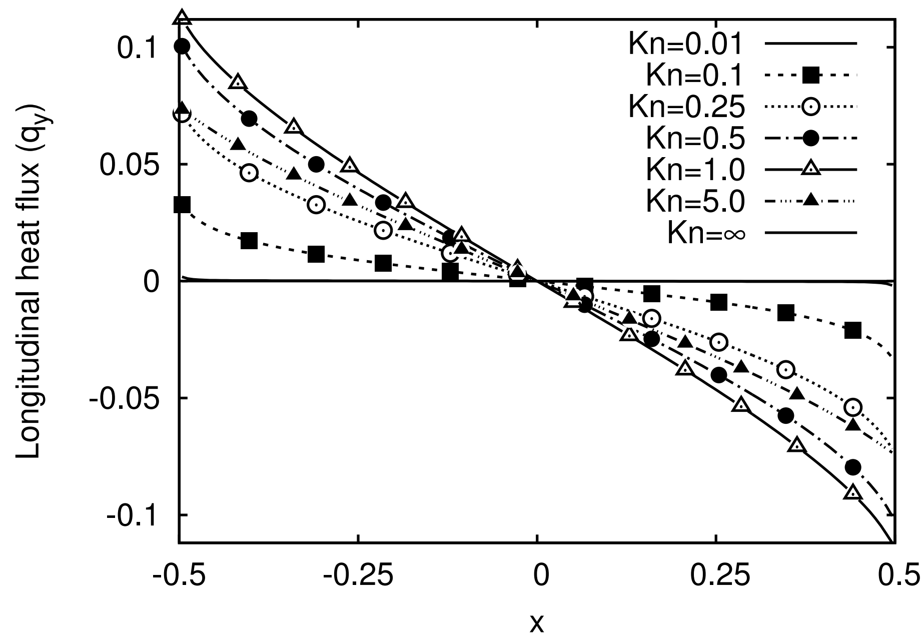

- At small Kn, $f \sim f^{(\mathrm{eq})}$ (according to C-E), so q_x and q_y vanish.
- $q_x^{\mathrm{ballistic}} = q_y^{\mathrm{ballistic}} = 0$.
- Reference profiles obtained using HHLB(21) $\times$ HLB(4).

V. E. Ambruș, V. Sofonea, J. Comp. Phys. **316** (2016) 1.

Dependence of $q_x(x_w)$ and $q_y(x_w)$ on Kn

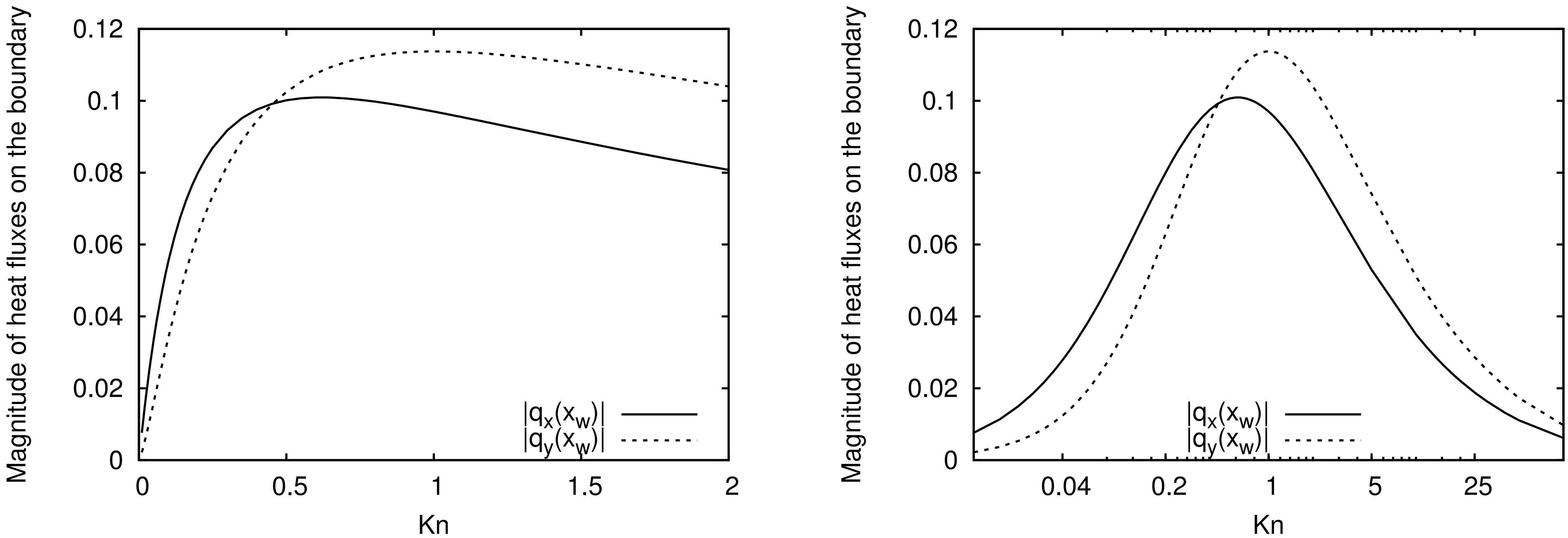

- Maximum of $|q_x(x_w)|$ and $|q_y(x_w)|$ at Kn $\simeq$ 0.62 and 1.0, in qualitative agreement with [29]
- Reference profiles obtained using HHLB(21) $\times$ HLB(4).

[29] Y. Sone, *Molecular Gas Dynamics: Theory, Techniques and Applications*, Birkhäuser, Boston, 2007.

Convergence of HHLB

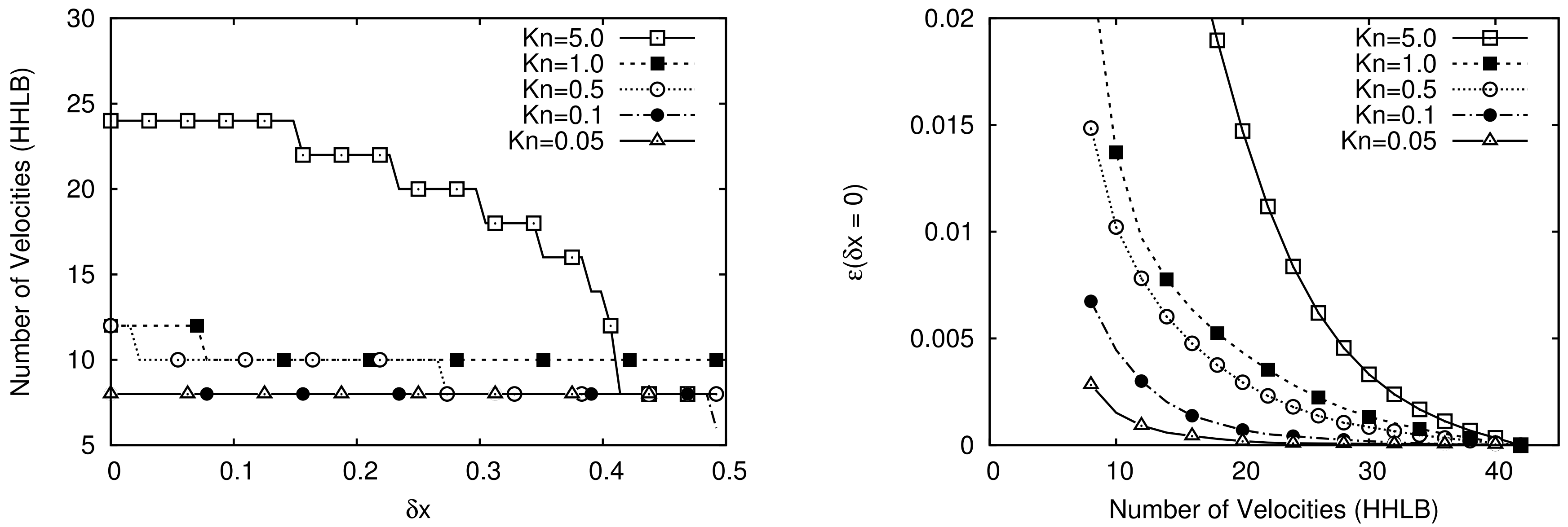

- $2D$ Couette-BGK ($u_w = 0.63$).
- The HHLB models exhibit fast convergence w.r.t. the increase in Q at all Kn.

V. E. Ambruș, V. Sofonea, J. Comp. Phys. **316** (2016) 1.

Convergence of HHLB over all Kn

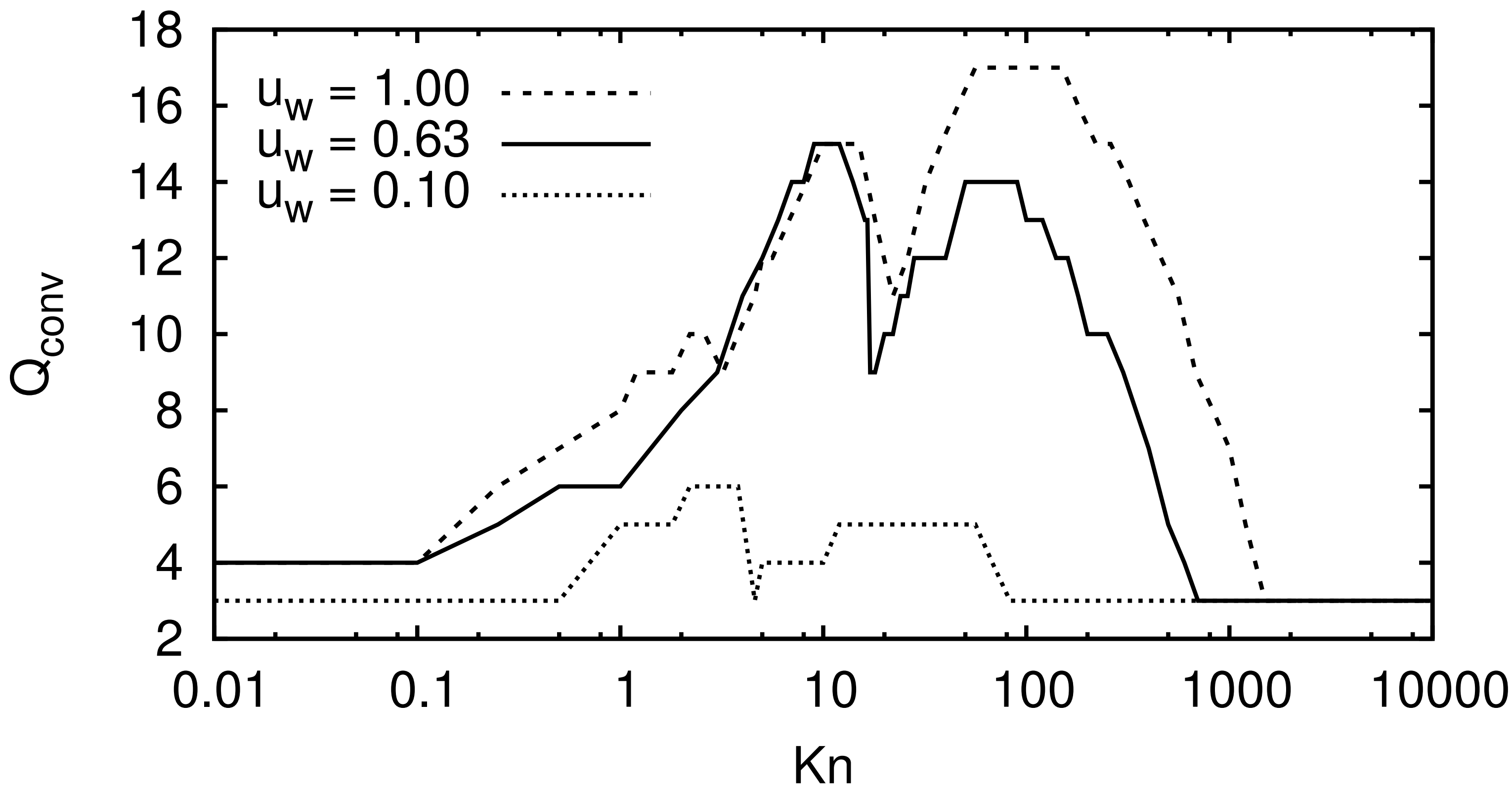

- The HHLB model was used to simulate the Couette flow over the whole $\mathrm{Kn} \in [10^{-4}, \infty)$.
- Good convergence was observed at all values of Kn and the results were validated against DSMC and linearised Boltzmann results at finite Kn, as well as against the analytical solution in the ballistic regime.

Force in Mixed LB models[30]

- For force acting along direction α:

$$f = \omega(p_\alpha) \sum_{\ell=0}^{\infty} \frac{1}{\gamma_\ell} \mathcal{F}_\ell \phi_\ell(p_\alpha), \qquad \mathcal{F}_\ell = \int dp_\alpha f \, \phi_\ell(p_\alpha),$$

  where $\mathcal{F}_\ell$ depends on all components of $\mathbf{p}$ except p_α.
- When the (full-range) HLB model is used on axis α, the Hermite force reads:

$$\nabla_{p_\alpha} f = -\omega(p_\alpha) \sum_{\ell=0}^{\infty} \frac{1}{\ell!} \mathcal{F}_\ell H_{\ell+1}(p_\alpha).$$

[30] V. E. Ambruș, V. Sofonea, J. Comp. Sci. (2016), http://dx.doi.org/10.1016/j.jocs.2016.03.016.

Poiseuille flow

- $2D$ flow between parallel plates ($x_+ = -x_- = -0.5$) subject to a constant acceleration $\mathbf{a} = (0, a, 0)$.
- Diffuse reflection on the x axis.
- $a = 0.1$, $T_w = 1.0$.
- Half-range models required to capture the discontinuous character of f.
- The reference profiles were obtained using the HHLB(21) $\times$ HLB(4) model.

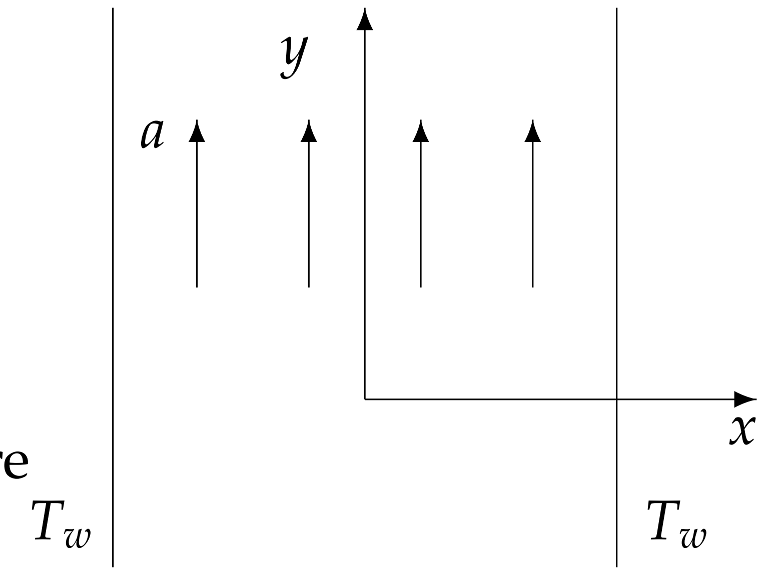

V. E. Ambruș, V. Sofonea, Phys. Rev. E **86** (2012) 016708 [3D, Shakhov]
V. E. Ambruș, V. Sofonea, Interfac. Phenom. Heat Transfer **2** (2014) 235–251 [3D, Shakhov]
V. E. Ambruș, V. Sofonea, J. Comp. Sci. (2016), http://dx.doi.org/10.1016/j.jocs.2016.03.016 [2D, BGK]

Validation

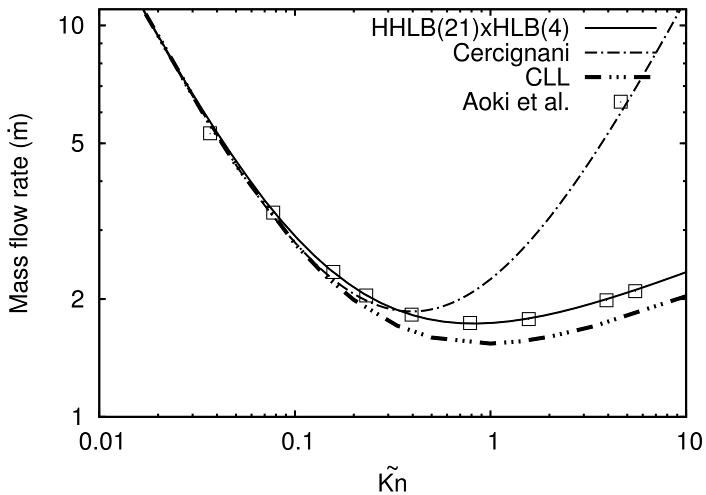

Mass flow rate

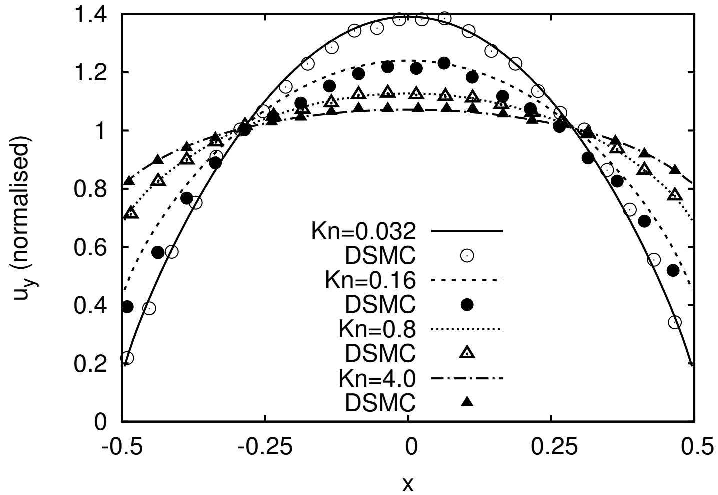

Velocity profile

- Comparison of mass flow rate against: analytic formula[31], CLL[32] and Aoki et al.[33].
- Comparison of velocity profiles against DSMC results from[34].

[31] C. Cercignani, *Theory and Application of the Boltzmann Equation* (Scottish Academic Press, Edinburgh, 1975).

[32] C. Cercignani, M. Lampis, S. Lorenzani, Phys. Fluids **16** (2004) 3426.

[33] K. Aoki, S. Takata, T. Nakanishi, Phys. Rev. E **65** (2002) 026315.

[34] S. H. Kim, H. Pitsch, I. D. Boyd, J. Comput. Phys. **227** (2008) 8655.

Temperature dip

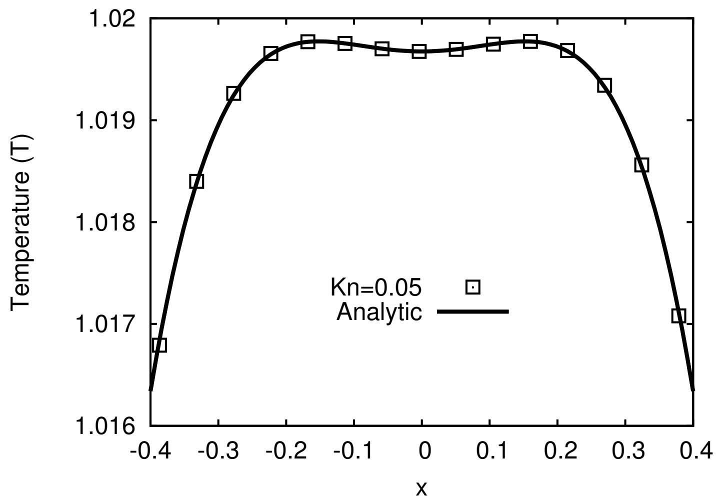

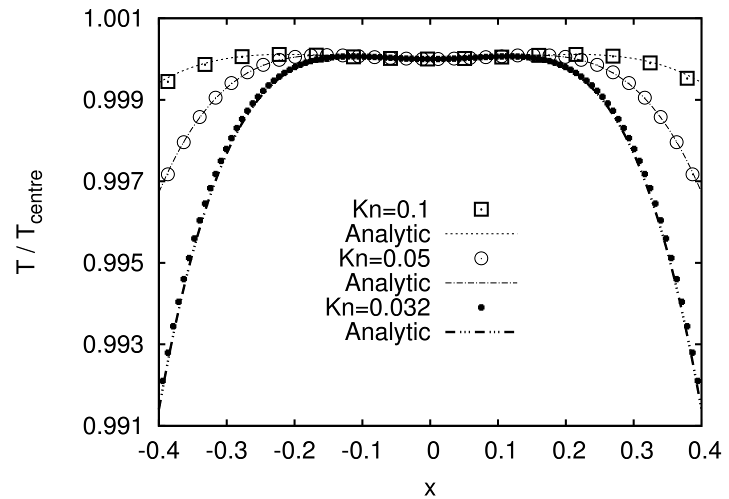

- Comparison with analytic formula[35] shows excellent agreement.

[35] S. Hess, M. M. Mansour, Physica A **272** (1999) 481.

Convergence of HLB vs. HHLB

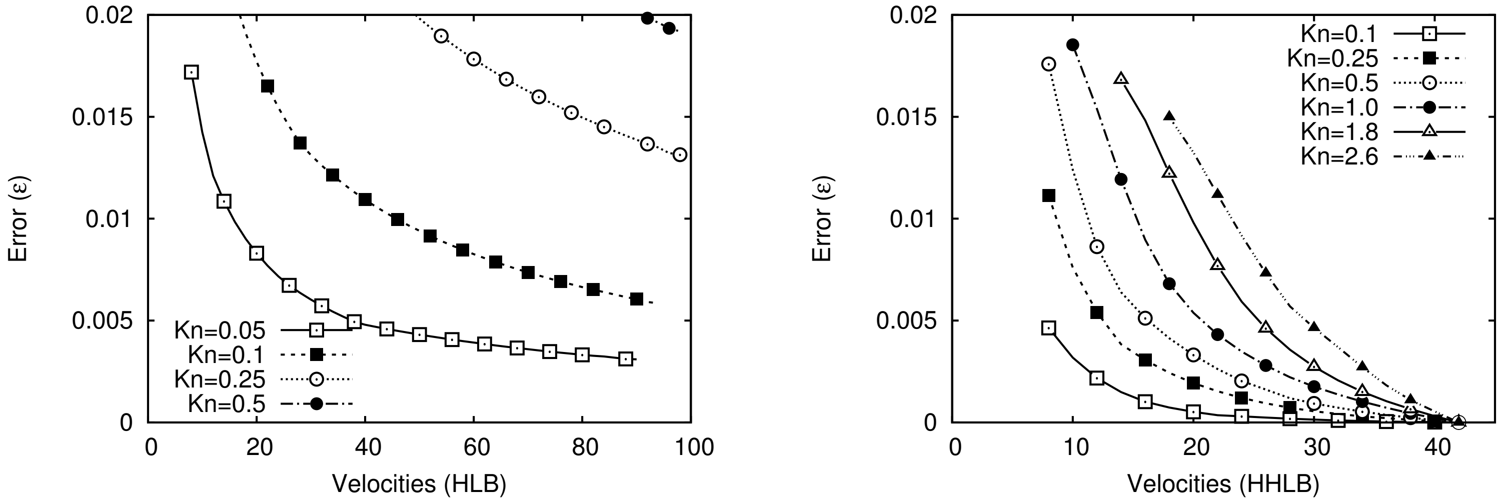

- The HHLB(Q_x) × HLB(4) models exhibit fast convergence.
- The HLB(Q_x) × HLB(4) models do not satisfy the 1% test for all $Q_x < 100$ when Kn $\gtrsim 0.25$.

Relativistic flows

- The Maxwell-Jüttner distribution describes the equilibrium state of non-degenerate gases:

$$f^{(\text{eq})} = \frac{n}{4\pi m^2 T K_2(m/T)} \exp\left(-\frac{p^0 u^0 - \mathbf{p}\cdot\mathbf{u}}{T}\right),$$

  where p^0 depends on $\mathbf{p}$ through the mass-shell condition $(p^0)^2 - \mathbf{p}^2 = m^2$.[36]

- The relevant moments of $f^{(\text{eq})}$ have space-time indices $\alpha, \beta, \dots \in \{0, 1, 2, 3\}$:

$$T_{\text{eq}}^{\alpha\beta\dots\gamma} = \int \frac{d^3p}{p^0} f^{(\text{eq})} p^\alpha p^\beta \dots p^\gamma.$$

- For massless particles ($p^0 = p$), quadrature rules can be applied in spherical coordinates:

$$\int \frac{d^3p}{p^0} f^{(\text{eq})} P(p^\alpha) = \int_0^\infty dp\, p \int d\Omega_p f^{(\text{eq})} P(p^\alpha).$$

[36] Planck units ($c = G = \hbar = 1$) are adopted for relativistic flows.

Quadratures for relativistic flows[37]

- The stress-energy tensor $T^{\mu\nu}$ can be obtained using the following integral:
$$T^{\mu\nu} = \int_0^\infty dp\, p^3 \int d\Omega_p f\, v^\mu v^\nu,$$
where $v^\mu = p^\mu/p = (1, \sin\theta\cos\varphi, \sin\theta\sin\varphi, \cos\theta)$.
- If only $T^{\mu\nu}$ is of interest, the Gauss-Laguerre quadrature with $\omega(p) = e^{-p}p^3$ can be used and only the 0'th order term in the expansion of f w.r.t. the $L_s^{(3)}$ polynomials needs to be retained.
- The angular integrals can be computed using the Myskovskih and Gauss-Legendre quadratures for the φ and θ integrals.

[37] P. Romatschke, M. Mendoza, S. Succi, Phys. Rev. C **84** (2012) 034903.

Expansion of $f^{(\mathrm{eq})}$

- The expansion of $f^{(\mathrm{eq})}$ can be writen as:

$$f^{(\mathrm{eq})} = e^{-p} \sum_{k=0}^{Q_p-1} \sum_{n=0}^{Q_\xi-1} a_{(nk)}^{i_1\dots i_n}(x,t) P_{i_1..i_n}^{(n)}\left(\frac{\vec{p}}{p}\right) L_j^{(1)}(p).$$

- For $T^{\mu\nu}$, $Q_p = 1$ and the sum over k is truncated at $k = 0$. The first few expansion coefficients $a^{(n0)}$ are:

$$a_{\mathrm{eq}}^{(00)} = \theta^4\left(1 + \frac{4}{3}\mathbf{u}^2\right), \qquad a_{\mathrm{eq}}^{(10)} = 4\theta^4 u^i u^0, \qquad a_{\mathrm{eq}}^{(20)} = 10\theta^4\left(u^i u^j - \mathbf{u}^2\frac{\delta_{ij}}{3}\right),$$

$$a_{\mathrm{eq}}^{(30)} = \frac{35\theta^4}{12\mathbf{u}^6} P_{ijk}^{(3)}(\mathbf{u})\left[u^0(15 - 10\mathbf{u}^2 + 8\mathbf{u}^4) - \frac{15}{2|\mathbf{u}|}\log(1 + 2\mathbf{u}^2 + 2|\mathbf{u}|u^0)\right].$$

- Cons: The quadrature does not give access to $N^\alpha = n u^\alpha$.

P. Romatschke, M. Mendoza, S. Succi, Phys. Rev. C **84** (2012) 034903.

Momentum set

- The resulting velocity set is comprised of the vectors

$$
\begin{aligned}
p^0_{ijk} =& p_k, \\
p^x_{ijk} =& p_k \sin\theta_j \cos\varphi_i, \\
p^y_{ijk} =& p_k \sin\theta_j \sin\varphi_i, \\
p^z_{ijk} =& p_k \cos\theta_j).
\end{aligned}
$$

- $k = Q_p = 1$ and $p_k = 4$.
- $1 \le j \le Q_\xi$ and $P_{Q_\xi}(\cos\theta_j) = 0$.
- $1 \le \varphi_i \le Q_\varphi$ and $\varphi_i = 2\pi(i-1)/Q_\varphi$.

Quadrature for N^α [38]

- Goal: quadrature to compute moments of f using:

$$T^{\alpha\beta\dots\gamma} = \int \frac{d^3p}{p^0} f\, p^\alpha p^\beta \dots p^\gamma = \sum_k f_k\, p_k^\alpha p_k^\beta \dots p_k^\gamma.$$

- Solution: use spherical coordinates, but employ Gauss-Laguerre quadrature with respect to $\omega(p) = e^{-p} p$:

$$\int \frac{d^3p}{p^0} f\, P_s(p^\mu) = \int_0^\infty dp\, p \int d\Omega_p f\, P_s(p^\mu).$$

[38] R. Blaga, V. E. Ambruș, Presentation at TIM-2016 conference (May, 2016), Timișoara, Romania.

Expansion of $f^{(\text{eq})}$

- $f^{(\text{eq})}$ is expanded w.r.t. $L_\ell^{(1)}$ and $P^{(n)}_{i_1\dots i_n}(\mathbf{v})$:

$$f^{(\text{eq})} = \frac{e^{-\bar{p}}}{4\pi T_0^2} \sum_{l=0}^{\infty} \sum_{n=0}^{\infty} \frac{1}{l+1} a^{(nl)}_{i_1..i_n} P^{(n)}_{i_1\dots i_n}(\vec{v}) L_l^{(1)}(\bar{p}),$$

- where the expansion coefficients are:

$$a^{(00)} = \frac{n}{2T_0\theta}, \qquad a^{(01)} = \frac{n}{T_0\theta}(1-\theta u^0), \qquad a_i^{(11)} = \frac{n}{T_0}(-3u^i),$$

$$a^{(02)} = \frac{n}{2T_0}\left[\theta\left(4(u^0)^2 - 1\right) + \frac{3}{\theta} - 6u^0\right], \qquad a_i^{(12)} = \frac{9nu^i}{T_0}\left(1 - \frac{2}{3}\theta u^0\right),$$

$$a_{ij}^{(22)} = \frac{15}{4}\frac{n\theta}{T_0}\left[\left(4u^i u^j - \delta_{ij}\right) - \frac{\delta_{ij}}{3}(4(u^0)^2 - 1)\right].$$

- At the moment, the coefficients $a^{(n>l,l)}$ are set to 0 (they are not necessary for the recovery of the moments of $f^{(\text{eq})}$).

The Riemann problem[39]

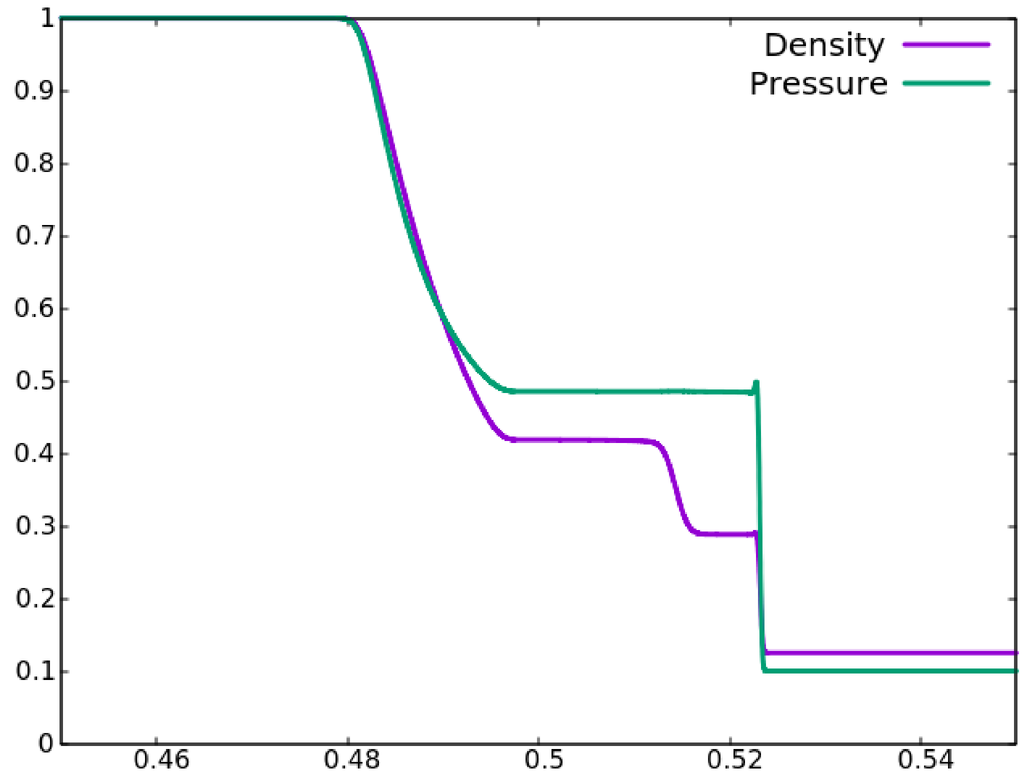

- The density profile exhibits (left to right): rarefaction wave, contact discontinuity, shock wave.
- The contact discontinuity is absent in the pressure profile.

[39] R. Blaga, V. E. Ambruș, Proceedings of TIM-2016 conference (May, 2016), Timișoara, Romania (work in progress).

The Riemann problem

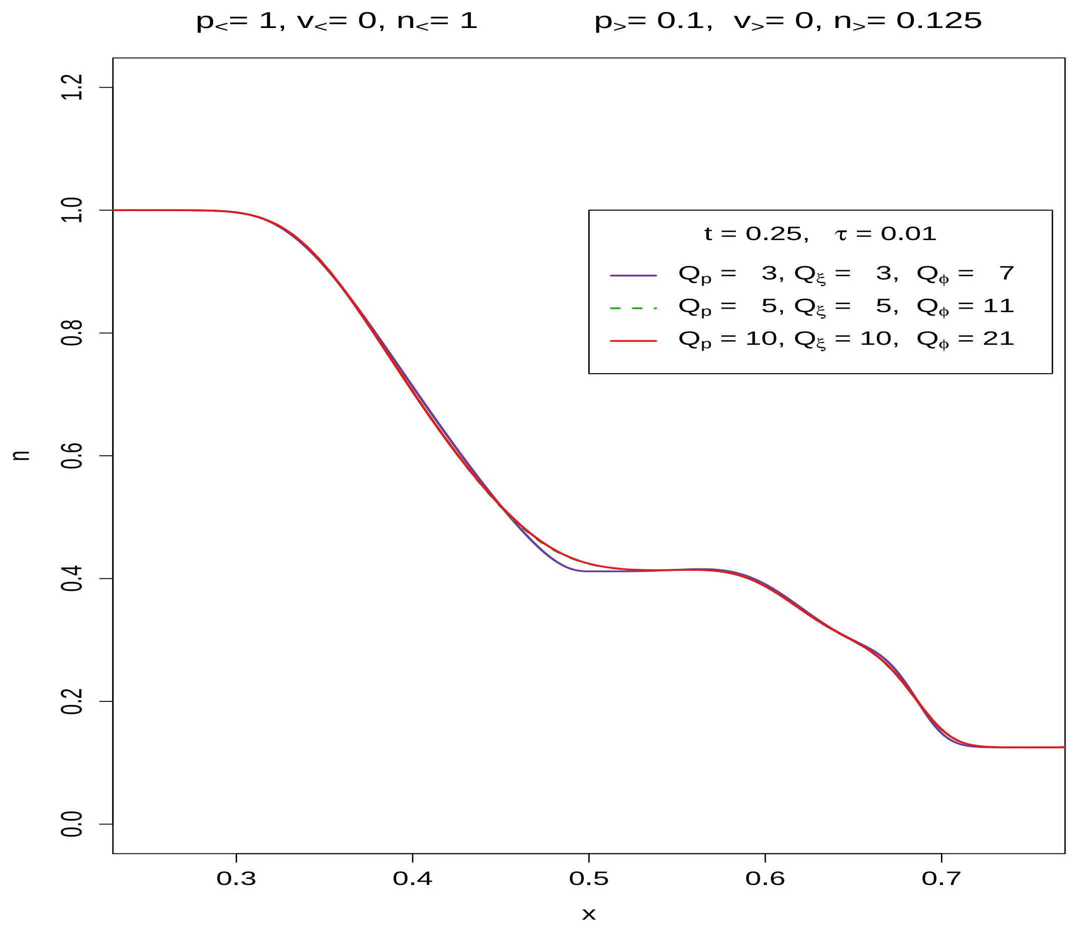

- The curves for $Q_p = Q_\xi = 5, 10$ are indistinguishable
- The procedure converges for increasing order of the quadrature

R. Blaga, V. E. Ambruș, Proceedings of TIM-2016 conference (May, 2016), Timisoara, Romania (work in progress)

Conclusion

- Quadrature methods provide recipes for the construction of LB models of arbitrarily high orders.
- Quadrature-based models are robust, showing good stability over large regions of the parameter space.
- Due to the nature of the roots of orthogonal polynomials, quadrature-based LB models are in general off-lattice, requiring finite difference or finite volume schemes to perform the advection step.
- Navier-Stokes level phase separation of van der Waals fluids shows good stability.
- Half-range quadratures show good efficiency for the simulations of rarefied gas flows up to the ballistic regime.
- Quadratures can be extended to relativistic flows.
- This work is supported by grants from the Romanian National Authority for Scientific Research, CNCS-UEFISCDI, project numbers: PN-II-ID-PCE-2011-3-0516, PN-II-ID-JRP-2011-2-0060, PN-II-RU-TE-2014-4-2910.